DIURNAL RESPONSE OF SHOOT GROWTH TO TREE WATER STRESS

By

EMILY ELAINE MASSEY

A THESIS PRESENTED TO THE GRADUATE SCHOOL
OF THE UNIVERSITY OF FLORIDA IN PARTIAL FULFILLMENT
OF THE REQUIREMENTS FOR THE DEGREE OF
MASTER OF SCIENCE

UNIVERSITY OF FLORIDA

2011

To my parents, Rhonda and Terry Massey

ACKNOWLEDGMENTS

The efforts of numerous people went into the formation, implementation, and completion of this thesis, and to them I owe many thanks.

First, I would like to thank Dr. Richard C. Beeson, Jr. for reading this manuscript and programming my irrigation time clocks. His expertise was greatly appreciated throughout the editing of this thesis. I would also like to extend my gratitude to my committee members Drs. Michael E. Kane and Timothy A. Martin for their support and manuscript review. I learned much about water relation techniques, plant physiology, and balance from all of them.

Second, I would like to extend thanks to Christopher Fooshee and Brian Pearson for their technical support, guidance, and statistical expertise. A special thanks also goes out to Edward Tillman, Cody Abston, Mark Jackson, and Steve Toomoth for their aid in the implementation and setup of my research. I would like to thank all staff and professors at the MREC and Dr. William MacKay for their kind words and inspiration.

Finally, I would like to acknowledge my family and friends for their support and encouragement with a special thanks to my parents, Marc Malone, Sarah Carls, and Tim and Becky Moss. I am especially thankful to Brandon Burmeister for all of his support and review of this manuscript as well.

TABLE OF CONTENTS

page

ACKNOWLEDGMENTS 4

LIST OF TABLES 7

LIST OF FIGURES 9

LIST OF ABBREVIATIONS 10

ABSTRACT 12

CHAPTER

1 INTRODUCTION 14

Water Potential 15
Water Balance in Plants 17
Water Movement from Soil to Roots 17
Water Movement in Xylem 18
Water Movement in Leaves 19
Plant Gas Exchange 19
Transpiration 19
Stomatal Conductance 19
Photosynthesis 21
Plant Growth 21
Plant Growth: Cell Wall Expansion and Turgor Pressure 22
Plant Growth: Turgor Pressure 23
Plant Growth: Elongation Rates 24
Irrigation Effects on Plant Growth 25
Water Stress 25
Water Stress Effects on Plant Growth 26
Maintenance of Turgor Pressure: Osmotic Adjustment 27
Water Stress Effects on Stomatal Aperture 28
Water Stress Effects on Photosynthesis 29
Quantification of Water Status, Gas Exchange, and Plant Growth 30
Pressure Chambers 30
Pressure-Volume Curves 30
Porometers and Infrared Gas Analyzers 33
Plants of Study 33
Quercus virginiana 33
Ulmus parvifolia 34

2 MATERIALS AND METHODS 38

Season One 38

Shoot Growth Measurements 40
Xylem Water Potential Measurements 40
Pressure-Volume Curves 41
Relation of Turgor Pressure to Shoot Growth 42
Leaf Gas Exchange Measurements 43
Season Two 43
Shoot Growth Measurements 45
Xylem Water Potential Measurements 45
Pressure-Volume Curves 45
Relation of Turgor Pressure to Shoot Growth 46
Statistical Analysis 46

3 RESULTS 55

Season One 55
Shoot Elongation Rate 55
Relation of Turgor Pressure to Shoot Growth 56
Pressure-Volume Curves 56
Leaf Gas Exchange 57
Season Two 58
Shoot Elongation Rate 58
Relation of Turgor Pressure to Shoot Growth 59
Pressure-Volume Curves 61

4 DISCUSSION 71

Seasons One and Two 71
Leaf Gas Exchange 71
Pressure-Volume Curves 73
Shoot Elongation Rate 77
Relation of Turgor Pressure to Shoot Growth 79

LIST OF REFERENCES 84

BIOGRAPHICAL SKETCH 92

LIST OF TABLES

Table		page
2-1	Tree fertilization schedule across Seasons One and Two.	48
3-1	Shoot elongation rates measured across a five day period for irrigation regimes across species.	62
3-2	Chinese elm shoot elongation rates measured across a five day period for irrigation regimes.	62
3-3	Interaction between species, irrigation regime, and time of growth for turgor pressure-normalized ($\Psi_{P\text{-}Norm}$) growth rate across species.	62
3-4	Interaction of species and shoot age for relative symplastic water content at incipient plasmolysis (SWC_{IP}) across species.	63
3-5	Interaction of irrigation regime and shoot age for relative symplastic water content at incipient plasmolysis (SWC_{IP}) across species.	63
3-6	Interaction of species and shoot age for osmotic potential at incipient plasmolysis ($\Psi\pi_{IP}$) across species.	63
3-7	Interaction of irrigation regime and shoot age for osmotic potential at incipient plasmolysis ($\Psi\pi_{IP}$) across species.	64
3-8	Interaction between species, irrigation regime, and shoot age for maximum turgor pressure (P_{max}) across species.	64
3-9	Interaction of irrigation regime and shoot age for bulk modulus of elasticity of Chinese elm during across irrigation regimes.	65
3-10	Interaction of species and shoot age for maximum modulus of elasticity (E_{max}) across species	65
3-11	Interaction of species, irrigation regime, and time of growth for shoot elongation across species.	66
3-12	Interaction of irrigation regime and time of growth for shoot elongation in live oak over the course of diurnal Ψ_w measurements.	66
3-13	Interaction of irrigation regime and time of growth for shoot elongation in Chinese elm	67
3-14	Interaction between species and time of growth for turgor pressure-normalized ($\Psi_{P\text{-}Norm}$) growth rate across species.	67

3-15 Interaction of irrigation regime and time of growth for turgor pressure-normalized ($\Psi_{P\text{-}Norm}$) growth rate in Chinese elm. 68

3-16 Interaction of species and shoot age for osmotic potential at incipient plasmolysis ($\Psi\pi_{IP}$) during Season Two across species. 68

3-17 Interaction of species and shoot age for maximum turgor pressure (P_{max}) during Season Two across species. 68

LIST OF FIGURES

Figure page

1-1 Photographs of *Quercus virginiana* taken in April 2011 at the Mid-Florida Research and Education Center in Apopka, Florida. 36

1-2 Photographs of *Ulmus parvifolia* taken in April 2011 at the Mid-Florida Research and Education Center in Apopka, Florida. 37

2-1 Open-side gutter-connected sawtooth style greenhouse located at the Mid-Florida Research and Education Center in Apopka, Florida. 48

2-2 Series of frequently irrigated trees (FI) 49

2-3 Series of lysimeter trees (LDI or $LDI_{2\text{-}Daily}$, or LLI). 50

2-4 Shoot age distinction of study trees for *Ulmus parvifolia*. 51

2-5 Shoot age distinction of study trees for *Quercus virginiana*. 51

2-6 Laboratory pressure-volume (P-V) curve station located at the Mid-Florida Research and Education Center in Apopka, Florida 52

2-7 Diurnal water potential (Ψ_x) and subsequently estimated turgor pressure (Ψ_p) of frequently irrigated (FI) live oak in Season Two 53

2-8 Diurnal water potential (Ψ_x) and subsequently estimated turgor pressure (Ψ_p) of frequently irrigated (FI) Chinese elm in Season Two. 54

3-1 Diurnal water potential (Ψ_x) and subsequently estimated turgor pressure (Ψ_p) of live oak in Season Two 69

3-2 Diurnal water potential (Ψ_x) and subsequently estimated turgor pressure (Ψ_p) of Chinese elm in Season Two. 70

LIST OF ABBREVIATIONS

$1/r_s$	Stomatal conductance
ρ_w	Density of water
Ψ_g	Gravitational potential
Ψ_l	Leaf water potential
Ψ_m	Matric potential
Ψ_p	Pressure or turgor potential
$\Psi_{P\text{-}Norm}$	Turgor pressure-normalized
Ψ_s	Osmotic potential
Ψ_T	Total water potential
Ψ_w	Water potential
Ψ_x	Xylem water potential
Ψ_z	Electrical potential
$\Psi\pi_{IP}$	Osmotic potential at incipient plasmolysis
A	Photosynthesis
ABA	Abscisic acid
E	Transpiration
E_o	Bulk modulus of elasticity
E_{max}	Maximum modulus of elasticity
EST	Eastern Standard Time
ET	Evapotranspiration rate
ET_A	Actual evapotranspiration rate
Exp. 1	Experiment 1
Exp. 2	Experiment 2
F	Faraday's constant

FI	Frequently irrigated
g	Gravity
g_s	Stomatal conductance
h	Height
hr	Hour
IRGA	Infrared gas analyzer
LDI	Once-daily well-irrigated lysimeter
$LDI_{2\text{-}Daily}$	Twice-daily well-irrigated lysimeter
LLI	Water limited lysimeter irrigation
LSD	Least Significant Difference
mm	Millimeters
MPa	Megapascals
Max-night	Maximum night
Min-night	Minimum night
P_{max}	Maximum turgor pressure
P_n	Photosynthesis
P-V	Pressure-volume
r_c	Cuticular resistance
r_i	Intercellular resistance
r_p	Stomatal pore resistance
SWC_{IP}	Relative symplastic water content at incipient plasmolysis
z_j	Charge

Abstract of Thesis Presented to the Graduate School
of the University of Florida in Partial Fulfillment of the
Requirements for the Degree of Master of Science

DIURNAL RESPONSE OF SHOOT GROWTH TO TREE WATER STRESS

By

Emily Elaine Massey

August 2011

Chair: Richard C. Beeson, Jr.
Cochair: Michael E. Kane
Major: Horticultural Science

Few studies have measured angiosperm shoot elongation, and fewer still have related elongation rates of trees to turgor pressure. The objective of this thesis was to quantify effects of turgor pressure on shoot elongation for two common Florida landscape trees, *Quercus virginiana* Mill. (live oak) and *Ulmus parvifolia* 'Allée'® Jacq. (Chinese elm). Methodologies were developed over a variety of irrigation regimes to measure and quantify turgor-pressure influenced growth rates.

Data were collected over two seasons. In Season One, higher nighttime turgor pressures were expected to result in higher nighttime shoot elongation rates. Shoots of well-watered trees elongated at rates 13 times higher than those of mildly water stressed trees. Elongation rates between day and night were similar. Turgor pressure-normalized growth rates were greater during the day than at night. In Season Two, measured shoot elongation rates were similar between day and night under well-watered conditions for both species. Timing of irrigation events segregated shoot elongation rates. For Chinese elm, regimes with night irrigation events produced greater growth rates than dawn-only, with rates similar between night and day within regimes.

For live oak, segregation occurred based on proximity to an irrigation event, with greater elongation occurring during the day or night period immediately after an event. Turgor-normalization accounted for these differences in growth rates in live oak. However turgor-normalized rates for Chinese elm were greater during day than at night within an irrigation regime, and did not correspond with turgor pressures. Results suggest a turgor pressure threshold in Chinese elm above which increases in shoot elongation rate do not occur, and that this threshold is low. Thus growth for some species is directly related to turgor, and this can account for differences in day and night shoot elongation. Differences between species in regards to turgor pressure-normalized growth rates may indicate cell wall loosening mechanisms also differ in live oak and Chinese elm. Further experiments should focus on validating this result. Results from this study are expected to influence irrigation scheduling for live oak and Chinese elm and add to knowledge of turgor pressures role in shoot elongation of these two species.

CHAPTER 1
INTRODUCTION

Plant growth is affected by internal physiological and chemical processes, which in turn are affected by a plant's environment. Soil and atmospheric conditions impact plant water status, and plant water status impacts turgor pressure in cells (Kramer and Boyer, 1995). Maintenance of turgor pressure is required for plant growth (Anderson and Brodbeck, 1988), with decreases in growth measured when substrate water availability is reduced (Ripullone et al., 2009).

Plant cell expansion is driven by two processes, which consist of the passive uptake of water and stress relaxation through biochemical inputs. These two processes interact in a continuous cycle of turgor-driven elastic extensions and biochemical stress relaxation until growth ceases (Taiz, 1994). Mechanisms involving cell wall expansion are currently under review with increasing knowledge being found as to the key players involved in cell wall-loosening. However, current measurements of cell wall extendibility are often hard to quantify *in vitro* given current methodology and the sensitivity of short-lived cell wall-loosening processes within cell wall spaces (Cosgrove, 2011).

While much is known about plant water relations and the physiology of plant growth, few studies have quantified diurnal plant growth rates. Fewer still have related measured growth rates to turgor pressure. The research presented here examined relationships between turgor pressure and shoot elongation of expanding shoots for two commonly grown landscape trees in the southeastern United States (*Quercus virginiana* and *Ulmus parvifolia*). Results of this study will guide both nursery producers and landscape managers in the scheduling of irrigation for optimum or reduced shoot growth.

Water Potential

Chemical potential is a measure of free energy available for work in a system, quantified in joules. It is governed by the two laws of thermodynamics and calculated from differences between a substance and the same substance in a standard state (Taiz and Zeiger, 2006).

Chemical potential is applicable to the movement of water in a plant when water is compared to its standard state. This value is also known as the water potential (Ψ_w) within a plant, and is the measure of free energy of water divided by water volume (Jm^{-3}) (Raven et al., 2005). Movement of water in plants is affected by gravity, osmosis, mechanical pressure, and/or matrix effects like surface tension. Total water potential measurements are made using psychrometers or pressure chambers because Jm^{-3} is equivalent to pressure units such as pascals (Nobel, 2009).

Typically in moist soils, diurnal water potential patterns in plants are U-shaped with Ψ_w close to zero at dusk and dawn and a maximum, negative midday level. For example, Koch et al. (1994) measured midday Ψ_w measurements between -2 and -3 MPa for five rain forest trees, and Cline and Campbell (1976) found similar results for maple (-2) and pine (-2.5 MPa) species.

Total water potential (Ψ_T) is a function of osmotic potential (Ψ_s), pressure potential (Ψ_p), matric potential (Ψ_m), gravitational potential (Ψ_g), and electrical potential (Ψ_z) where $\Psi_w = \Psi_s + \Psi_p + \Psi_m + \Psi_g + \Psi_z$ (Raven et al., 2005).

Osmotic potential is the potential of water molecules to move across a semipermeable membrane. Its magnitude depends on solute concentration because solutes lower the chemical potential of water. Free movement of water generally occurs from hypotonic solutions (*i.e.,* solutions with more water than solutes) to hypertonic

solutions (*i.e.,* solutions with more solutes than water) or from areas of high to low water potential (Lambers et al., 2008) . Osmotic potential can be measured directly using osmometers (Nobel, 2009).

Pressure potential (Ψ_p) is pressure exerted by water against cell walls. Pressure potential is affected by Ψ_w and Ψ_s gradients within plants cells. Turgidity is sustained in plants when ions, sugars, and other solutes accumulate in cell vacuoles. Solute accumulation lowers Ψ_w, causing an influx of water into cells and an increase in rigidity (Lambers et al., 2008). Turgor pressure maintenance is important for many plant processes (*i.e.,* stomatal aperture, plant growth, and negative values or tension help pull water through xylem vessels) and is measured using pressure probes or calculated from pressure-volume curves (P-V curves) (Nobel, 2009).

Matric potential is a measure of how strongly water is held in soil pores and within cell walls and spaces. It is particularly large for dry surfaces and small surface areas (*i.e.,* cell wall spaces and soil pores) where adhesion (*i.e*., the attraction of water to the surfaces of other objects) is strong. When adhesive forces are strong, the number of water molecules available for free movement is decreased, lowering water's chemical potential (Lambers et al., 2008). Matric potential is measured using tensiometers and pressure plates (Kramer and Boyer, 1995). Gravitational potential is generally only considered for tall plants like mature trees. It is a product of the density of water (ρ_w), acceleration due to gravity (g), and plant height (h) with a vertical distance of 10 m equaling a change of about 0.1 MPa in Ψ_w (Taiz and Zeiger, 2006). Electric potential is the amount of work required to move an electrical charge, and it is consideration when ions are present in a solution. Electrical potential is a product of charge (z_j), Faraday's

constant (F), and electric potential difference across the membrane at equilibrium (Nobel, 2009). Generally, matric and gravitational potentials are ignored from water potential equations for predicting water movement in short plants, given their negligible impact when compared to the impacts of Ψ_s and Ψ_p, and Ψ_z becomes important only when ions are present.

Water Balance in Plants

In addition to internal processes, the environment external to plants has a major impact on plant water balance. The plant-water cycle begins with water movement through soil and ends with water vapor exiting plant stomata into the atmosphere (Lambers et al., 2008). This cycle is driven by transpiration and is explained by the cohesion-tension theory. In this theory, tension, along with cohesive (attraction of water to other water molecules) and adhesive properties of water, creates a pull on water from the soil into plant roots and throughout the plant (Taiz and Zeiger, 2006).

Water Movement from Soil to Roots

The plant-water cycle begins in the soil. Water movement in soils depends on soil type and structure because components of soil determine pore spaces sizes and channels between individual particles of soil. Movement of water in soils is dictated by Ψ_s and hydrostatic pressure, with the former being normally negligible due to the low solute concentrations in soils (Kramer and Boyer, 1995). As water is depleted from soils, adhesion increases between water and soil particles and water becomes increasing harder to remove from soil.

Water transport into roots occurs via passive transport due to negative hydrostatic pressure generated by transpiration and water potential gradients across tissues. Root hairs increase surface area available for water absorption. Movement of water through

root tissue occurs through two pathways: apoplastic (*i.e.,* movement through intercellular spaces) or symplastic (*i.e.,* movement through spaces within cellular membranes via plasmasdesmata and aquaporines) (Nobel, 2009). Plasmodesmata and aquaporins are more efficient than osmosis through lipid bilayers (Taiz and Zeiger, 2006). Plasmodesmata are microscopic membrane lined channels connecting neighboring cells (Raven et al., 2005). Aquaporins are water selective channels consisting of proteins embedded in plasma membranes, which facilitate active transport of water into cells (Taiz and Zeiger, 2006).

Water Movement in Xylem

Once water transverses the root cortex, it travels through an extensive number of hollow, dead tubes called tracheids and/or vessel elements. Flow of water through this path encounters little resistance and is driven by negative hydrostatic pressure gradients generated by leaf transpiration (Kramer and Boyer, 1995). However, large generated tensions in xylem may cause weakened cell walls to collapse or lead to increases in air bubble formation or embolisms. Embolisms lead to cavitation (*i.e.,* breaks in water continuity transport through xylem tissue). Many mechanism have evolved in plants to cope with these situations (*i.e.,* constant formation of new xylem in a secondary growth and development of pit membranes in vessel elements) (Lambers et al., 2008).

Capillary rise also contributes to water flow through xylem tissue. Xylem narrows as water flows up a tree through the wood, branch junctions, and leaf venation. This narrowing of the xylem coupled with surface tension and water's cohesive and adhesive properties allows for water to flow against gravity (Taiz and Zeiger, 2006).

Water Movement in Leaves

Water exits xylem elements in leaves and moves into mesophyll cells and intercellular air spaces using a process similar to water movement in soils. Water moves into substomatal cavities and exits stomata as water vapor via Ψ_w gradients generated by relative water vapor pressure differences between leaf substomatal cavities (~100% relative humidity) and bulk air, completing transpiration (Lambers et al., 2008).

Plant Gas Exchange

Transpiration

Transpiration is affected by conditions external to (*i.e.,* relative humidity and temperature) and within leaves. Boundary layer resistance also affects transpiration. Boundary layer resistance is related to length of water vapor diffusion due to a layer of unstirred air adjacent to the leaf surface. Resistance generated from boundary layers is proportional to layer thickness. It is dependent on wind speed; canopy thickness; and leaf size, shape, and surface. Resistances within plant leaves are cuticular (r_c) and stomatal (r_s) (*i.e.,* sum of intercellular space (r_i) and stomatal pore (r_p) resistances) (Kramer and Boyer, 1995).

Stomatal Conductance

Stomatal conductance (g_s) is a measure of flux rate of water vapor inside a leaf through a leaf's surface to the outside, normalized by the water vapor pressure difference between the two end points. Stomatal conductance, which is equivalent to the inverse of stomatal resistance, is a function of stomatal density and stomatal aperture, which is controlled by Ψ_p in plant guard cells (Kramer and Boyer, 1995). Generally stomata open at dawn when photoreceptors in guard cells are activated by

blue light. This activation triggers an increase in potassium concentration and water flows into guard cells increasing turgidity and stomatal aperture (Taiz and Zeiger, 2006). As water vapor escapes through open stomata, carbon dioxide diffuses into plant leaves. Patterns for g_s follow an inverted U-shape with levels at dawn and dusk at zero and maximum levels peaking around midday (Wullschleger et al., 2000). Water loss usually peaks around midday in response to maximum vapor pressure gradients, triggering stomatal closure in isohydric tree species (Tardieu and Simonneau, 1998). Carbon dioxide assimilation begins to slow as stomatal aperture decreases (Larcher, 1980). In anisohydric tree species, stomatal aperture remains wide and closure is not triggered until Ψ_w rates approach a maximum negative value (Tardieu and Simonneau, 1998). Isohyrdric and anisohydric are terms used to describe the extent of tissue hydration under changing environmental conditions. Typically, isohydric plants have great control over transpiration rates, and anioshydric plants are less sensitivity to transpiration rates (Franks et al., 2007). This value varies by species. By dusk, most, if not all stomata are closed in response to declining light levels. Guard cells close and carbon assimilation ceases (Raven et al., 2005).

Stomatal conductance not only varies diurnally and in response to environmental factors, but also among species. Stomatal conductance of 140-316 mmol m^{-2} s^{-1} were measured in *Eucalyptus pauciflora* over a three month period (Korner and Cochrane, 1985). Gallego et al (1994) reported g_s of around 150-200 mmol m^{-2} s^{-1} for *Quercus pyrenaica*. Andrade et al (1998) found similar rates to those of *Q. pyrenaica* in *Ficus insipida*, *Luehea seemannii*, and *Spondias mombin* (178-211 mmol m^{-2} s^{-1}); with lower rates in *Anacardium excelsum* and *Cecropia longipes* (35-125 mmol m^{-2} s^{-1}). Stomatal

conductance varied depending on propagation method for *Ulmus glabra* (~51-98 mmol m^{-2} s^{-1} for micropropagted and grafted species, respectively) (Durkovic et al., 2010)

Photosynthesis

In plants, a balance between minimizing water loss by transpiration and sustaining carbon dioxide diffusion for assimilation is controlled by stomatal aperture. Assimilation of carbon dioxide, in part, determines photosynthetic (A) rates in autotrophic organisms. Photosynthesis is the process by which the sun's energy is converted to chemical energy in plant chloroplasts (Raven et al., 2005). Carbohydrates produced during A are important for biomass accumulation and growth in plants (Taiz and Zeiger, 2006).

Diurnal photosynthesis (µmol m^{-2} s^{-1}) patterns resemble those of g_s, with A being close to zero at dawn and dusk and maximum A occurring just prior to midday. Maximum net photosynthetic rates were measured at ~22 µmol m^{-2} s^{-1} for *Picea abies* and ~16 µmol m^{-2} s^{-1} for *Quercus pubescens*, respectively (Haldimann et al., 2008; Maier-Maercker, 1998). Photosynthesis for three year old grafted and micropropagated *Ulmus glabra* were ~33 and 23 µmol m^{-2} s^{-1}, respectively (Durkovic et al., 2010).

Plant Growth

Plant growth is defined as irreversible enlargement of cells (Hsiao et al., 1976). Growth consists of cell division and cell elongation. Cell division occurs when a parent cell divides into two or more daughter cells. Mitotic processes result in production of cells. Mitosis consists of five distinct phases: interphase, prophase, metaphase, anaphase, and telophase. Cytokinesis is the final step to this process (Raven et al., 2005). During cell elongation, plant cells can enlarge from 10 to 10,000 fold in volume from meristematic to mature cells depending on their function. Factors influencing cell expansion are cell type, age, auxin and gibberellin concentrations, and environmental

conditions such as light levels and water availability (Taiz and Zeiger, 2006). Two processes must take place for plant elongation to occur. First, water must be taken up by the elongating cells. Second, cell wall area must increase.

Plant Growth: Cell Wall Expansion and Turgor Pressure

Restriction of growth is typically caused by plant cell walls. Cell walls of plants consist of cellulose microfibrils embedded in a matrix of pectin, hemicellulose, and proteins (Taiz, 1994). However cell walls of growing cells are typically less ridged than those of non-growing cells. Stress relaxation is the key to cell wall expansion. First, turgor pressure inside cells increases as water flows into growing plant cells from adjacent cells due to water potential gradients. This increase in pressure creates a strain or tension to build up in cell walls. This strain is relieved through stress relaxation via biochemical input (Taiz, 1994).

Wall loosening enzymes are thought to be triggered by low pH in the cell walls, which is promoted in these areas by the presence of auxin-induced protein extrusion. These enzymes cleave components of the cell wall matrix and allow cell wall extension (Hager et al., 1971; Rayle and Cleland, 1970). Initially, hydrolases (*i.e.*, cellulases, hemicellulases, and pectinases) were thought to be the enzymes responsible for cleaving of bonds within the cell wall, but now transglycosylases such as xyloglucan endotransglycosylase are thought to be the primary enzymes involved. Transglycosylases are thought to be key players in elongation due to their ability to lay down cellulose in a biased orientation as bonds are systematic weakening between cell wall polymers of load bearing walls (Bonner and Varner, 1976; Carpita and Gibeaut, 1993; Fry, 1989; Fry et al., 1992; Smith and Fry, 1991). Later studies focused on one particular protein termed expanins, which appeared to induce cell wall extension. Like

hydrolases and transglycolases, expansins are activated by low pH. However unlike hydrolases, expansins extend cell walls without causing time-dependent weakening (Cosgrove, 1989). Expansins are thought to disrupt hydrogen bonds between cellulose fibers, causing slippage to occur between cellulose microfibrils and the polysaccharide matrix. As this slippage occurs, polysaccharides shift their positions in response to the orientation of cellulose microfibrils and this creates the formation of new hydrogen bonds to form, decreasing stress in cell walls (McQueen-Mason and Cosgrove, 1994; Taiz, 1994).

Various research has outlined ways to measure cell wall mechanics of growing plant cells (Burgert, 2006; Cosgrove, 2011; Geitmann, 2006). Extensibility is measured by extending a clamped specimen in various ways while recording cell wall behavior. These processes are typically carried out in a extensometer (Cosgrove, 1993; Geitmann and Ortega, 2009). However, despite the efforts of these studies, cell wall extensibility cannot be fully measured *in vitro* due the fact that cell wall extensibility is a multifaceted process consisting of cell wall mechanics, which can be inferred from extendibility, and wall-loosening processes. The latter is hardest to measure because cell wall loosening processes are influenced by short-lived conditions within cell walls, which may be further dependent on plant species and plant environment (Cosgrove, 2011).

Plant Growth: Turgor Pressure

Studies indicate that turgor must be maintained for growth to occur. Anderson and Brodbeck (1988) found in newly expanding flushes in pecans that leaf elongation rate was exponentially related to turgor pressure with maximum leaf elongation occurring at higher, overnight turgor pressures. Furthermore, Zwack et al. (1998) found when three Freeman maple cultivars were exposed to drought conditions that relative shoot

extension growth decreased in the morning and increased during the afternoon. Bulk turgor pressure seems to play less of a role in elongation in many non-woody species. Leaf elongation of maize and sorghum was lower during higher nighttime turgor pressures. This slower elongation rate was attributed to temperature (<12 C) and not necessarily Ψ_p because early in the morning they saw a noticeable increase in leaf elongation despite a decreasing Ψ_p (Acevedo et al., 1979). Leaf elongation rates in rice were also greater during the daytime, despite a lower bulk turgor during the daytime, when nighttime temperatures fell below 27^{o}C. When nighttime temperatures were above this temperature threshold, nighttime elongation was greater (Cutler et al., 1980).

Plant Growth: Elongation Rates

Few studies have reported short-term, diurnal shoot growth rates (mm hr^{-1}), and of those conducted there appears to be great variability in growth rates among species. Borchert (1976) measured pin oak sapling growth rates of 0.7917 mm hr^{-1}. Reich et al. (1980) measured stem height growth rates from 0.0164 to 0.0424 mm hr^{-1} in blackjack oak seedlings. Field grown *Zea mays* leaf elongation rates fluctuated diurnally (0.4 to 3.6 mm hr^{-1}) with minimal rates occurring from 0000-0500 hr (10-12 C) and maximal elongation at 1200 hr (32.5 C). Rates of growth can vary throughout a growing season depending on the plant species. Kramer (1943) reported that growth of young *Fraxinus americana*, *Juglans nigra*, *Quercus alba*, and *Q. borealis* in North Carolina occurred in recurrent waves (eposidial), whereas, some tropical evergreen tree species continuously produce new growth throughout the growing season (Koriba, 1958).

In addition to variable growth rates, much debate exists over daily diurnal patterns of shoot elongation. Studies of spruce, pine, and pecan indicate that shoot and leaf elongation occurred mostly at night (Anderson and Brodbeck, 1988; Fielding, 1955;

Mork, 1941), while other studies of woody species, maize, and sorghum indicated that a majority of shoot growth occurs during the day (Acevedo et al., 1979; Danilov, 1954).

Irrigation Effects on Plant Growth

Many studies have sought to maximize growth and marketability of plants by optimizing irrigation regimes. Beeson (1992) showed *Rhododendron* sp. and *Elaeagnus pungens* cyclically irrigated to 100% container capacity produced significantly greater growth than plants overhead irrigated once per day. Cyclic irrigation also increased rates of height growth and trunk diameter in *Magnolia grandiflora* compared to plants irrigated once per day (Beeson and Keller, 2003). Amounts of water supplied during irrigation also affect plant growth. Doubling irrigation volumes significantly increased growth of *Acer rubrum* and *Lagerstroemia indica* compared to plants overhead irrigated and plants micro-irrigated using 50% of the overhead irrigation volume (Beeson and Haydu, 1995). These results suggest direct spray stake irrigation and cyclical irrigation increased substrate water availability for plants throughout the day, maintaining a less negative plant water potential and therefore likely higher turgor pressures. This in turn led to increased plant growth rates.

However these experiments examined irrigation regimes implemented during the day. Irrigation at night has been shown to offset some of the reduction in growth due to decreased substrate water availability and may lead to increased water efficiency (Yacoubi et al., 2010) and growth in plants due to higher nightly turgor pressures (Anderson and Brodbeck, 1988).

Water Stress

Water stress occurs when plants are unable to absorb adequate amounts of water due to environmental or physiological constraints. Irrigation is often supplied to plants

to mitigate water stress or put an end to it. Water stress can be a result of drought, increased salinity of soils, and under-irrigation. Wilting occurs when plants lose water pressure of turgidity and it is common sign of water stress. When plants receive inadequate amounts of water, problems may arise such as hormonal, biochemical, or physiological changes; the production of fewer or smaller leaves; lower crop yields; a slowing or decrease growth in shoot growth; or death (Simpson, 1981).

Water Stress Effects on Plant Growth

The process most sensitive to water stress is cell growth, consisting of cell division and cell enlargement, of which the latter is the most affected in plants (Hsiao and Acevedo, 1974). Enlargement occurs through uptake of water. When plants experience water stress, water uptake may slow and growth may be retarded or stop in response to lower water potentials and a loss of turgor pressure (Lockhardt, 1965). However, decreases in growth are often dependent on stress severity and plant species. Zwack et al. (1998) reported that leaf elongation was lower for drought stressed Freeman maple cultivars (19 to 87 cm for drought and control trees, respectively). While other studies suggest water stress may vary among species and growth patterns. Lotan and Zahner (1963) found late-summer drought had no significant effect on *Pinus resinosa* height during the current season of growth. Whereas, Zahner (1962) found late-summer drought significantly reduced the number of growth flushes and height of *Pinus taeda*. Kozlowski (1982) suggested this is species mediated where plants with one fixed growth cycle exhibit affects in the subsequent growth season, and plants with recurrent flushes tend to exhibit effects in the same growth season.

Several species of pines and oaks exhibit mechanisms to counteract a loss in turgor (Danilov, 1954; Kozlowski, 1964). For instance, Bahari et al. (1985) found that under drought stress, several oak species displayed restricted leaf conductance and lower Ψ_s at full turgor. Growth of leaves and shoots are particularly susceptible to cessation for many species during periods of water deficit; however, roots are more variable with either slowing or slight increase in growth occurring (Raper and Kramer, 1983; Xu et al., 2006).

Maintenance of Turgor Pressure: Osmotic Adjustment

When water loss exceeds water supply and cell water volume decreases, loss of cellular turgor may result and plant processes other than growth may be affected, such as reduction in stomatal aperture and metabolic processes. Osmotic adjustment can maintain turgor pressure in plant cells. Osmotic adjustment is characterized by an increase in the concentration of solutes such as potassium, amino acids or amino acid derivatives, and/or sugars in cell vacuoles (Kramer and Boyer, 1995). Increased solutes lower osmotic potential, which results in a lower Ψ_w within the cells. The resulting water potential gradient between the cells and adjacent xylem causes an influx of water into the cells and allows for turgor to be maintained (Lambers et al., 2008). Osmotic adjustment initially occurs from starch and other components of the cell (Kramer and Boyer, 1995) with later solutes accumulated through photosynthesis (Wang and Stutte, 1992).

Many studies have shown that osmotic adjustment may be a response to water stress in plants. Species of oak, pine, and rapeseed were able to maintain turgor longer through the accumulation of higher concentrations of solutes in the roots and shoots of water stressed species (Osonubi and Davies, 1978; Koppenaal, et al., 1991; and Meier,

et al., 1991; Norouzi, et al., 2008). Osmotic adjustments in leaves and the roots of three species of oak reduced maximum Ψ_s in leaves of these species by 0.25 to 0.60 MPa (Parker and Pallardy, 1988).

Some suggest that these changes in Ψ_s shifts of oaks are not due to water stress, but due to seasonality or phenological responses with plants constantly undergoing changes to maintain biochemical and physiological balances in order to more efficiently operate (Abrams, 1990). Kwon and Pallardy (1989) looked at chronic stress on three oak species. Their data indicate that solute accumulation for some species of oaks may be limited under persistent water deficit.

Water Stress Effects on Stomatal Aperture

Another process affected by water stress in plants is stomatal aperture. Typically this process is not as sensitive as processes involved in plant growth (Hsiao and Acevedo, 1974). Effects of water deficit on gas exchange and subsequent effects on Ψ_w have been well documented for non-woody and woody species. Generally plants close stomata to minimize water loss during stress and maintain an adequate water status. Stomatal aperture is mediated by availability of moisture in soils and vapor pressure of the air. Closure begins to take place prior to water stress in leaves. In drying soils, it can be initiated by root signaling via translocation of abscisic acid (ABA) from plant roots to leaves. If a suitable water status can be maintained, preservation of turgor may persist and wilt may be avoided (Lambers et al., 2008). Abscisic acid also is implicated in other plant processes and is not solely synthesized in the roots of plants.

As soil water becomes limited, xylem water potentials (Ψ_x), measured at the leaf level also decrease (Mazzoleni and Dickmann, 1988). Under a prolonged water deficiency (25 days) leaf water potential (Ψ_l) and g_s for young oak seedlings declined

sharply (Fort et al., 1997). A decrease in Ψ_l was similarly found in three *Fagaceae* species during the peak drought period (Abrams et al., 1990). Water stress may lead to full or partial stomatal closure with the severity mediated by species and environmental conditions.

Water Stress Effects on Photosynthesis

While stomatal closure minimizes water loss, a decrease in carbon assimilation and subsequent photosynthetic rates may also result. Studies have also shown that when stomates close, or when turgor in plants is low, carbon dioxide in the sub-stomatal cavity decreases (Omae et al., 2007). Decreases in carbon dioxide mean plants will have a reduced photosynthesis rate. During a water reduction experiment, Gu et al. (2007) demonstrated a strong relationship in the reduction of g_s and P_n rates for four birch genotypes. Decreased evapotranspiration rates (ET), g_s, and P_n rates were also measured in four drought stressed oleander clones (Niu et al., 2008).

Reduced carbon fixation will limit biomass accumulation in most cases and plants may allocate less carbon and assimilates towards growth. Water deficits lead to a slowing of shoot elongation and often an inhibition or slight increase in root elongation through a variety of mechanisms (Raper and Kramer, 1983). Other studies indicate that a majority of fixed carbon is allocated to root elongation over elongation of shoots. A decrease in water availability reduced shoot dry weight and increased root dry weight for three grass seedlings (Xu et al., 2006). Decreases of 15-20% in precipitation reduced shoot elongation of plants in a Mediterranean macchia due to increased hydraulic resistance in the soil-plant continuum (Ripullone et al., 2009).

Quantification of Water Status, Gas Exchange, and Plant Growth

Pressure Chambers

Pressure chambers are devices used to measure xylem water potential (Ψ_x) in plants. Leaves or shoots are typically severed from plants and placed inside an airtight pressure chamber with petioles or stems exposed outside through a seal. Compressed gas, typically nitrogen, is forced into a chamber until water appears at the cut end of the exposed tissue. Pressure amounts inside devices are indicated on a gauge. This device works because water in plant xylem is under tension. When samples are collected, water within xylem recedes deeper in the sample. As pressure is increased in a chamber, water is forced from the sample to the cut end if the stem. The corresponding pressure is equal and opposite to tension within the sample at this time (Nobel, 2009).

Pressure-Volume Curves

Water parameters in plants can be assessed using pressure-volume (P-V) curves. Pressure-volume curves relate changes in Ψ_p and Ψ_s to changes in Ψ_x (Nobel, 2009). Curves are constructed using pressure chambers and plant structures such as leaves, shoots, or roots (Dreyer et al., 1990; Husken et al., 1978; Kandiko et al., 1980). Tissue removed from plants is fully hydrated shortly after removal, and periodic measurements of weight and balancing pressure readings are taken as the tissue is dehydrated past the turgor loss point. Dehydration can be caused by evaporation or by incrementally expressing xylem sap by subjecting the tissue to increased pressures. Reciprocals of balancing pressure are calculated and plotted against a measure of the tissue water content or volume (Abrams, 1988b). Pressure-volume curves are often

used to estimate relationships between Ψ_w components and water tissue contents (Tyree and Jarvis, 1982).

Some of these components include effects of turgor pressure on cell size and elasticity (Steudle et al., 1977). Other parameters can also be ascertained like symplastic water content. This is a measurement that quantifies amounts of water in the symplast, the space within the plasma membrane of the living cells (Nobel, 2009). Values of 0.81, 0.73 to 0.84, 0.69 to 0.86, 0.77 and 0.82 have been measured in shoots of *U. parvifolia*, leaves of *Juglans nigra*, leaves and shoots of *Q. alba*, expanding leaves of 'Colt' cherry, and mature leaves of 'Colt' cherry, respectively (Kandiko et al., 1980; Parker and Pallardy, 1985; Parker and Pallardy, 1987; Ranney et al., 1991; Ranney et al., 1990). A related parameter is the percentage of apoplastic water, which is a measurement that quantifies the percentage of water within the apoplast or outside plasma membranes and in the intercellular cell spaces (Raven et al., 2005).

Relative symplastic water content represents amounts of water within intracellular spaces when cells are fully turgid. Values of 0.84 have been measured in 'Colt' cherry for expanding and mature tissue (Ranney et al., 1991), 0.78 to 0.83 in leaves and shoots of *Q. alba* (Parker and Pallardy, 1987), and 0.81 in *U. parvifolia*, respectively (Ranney et al., 1990). Whereas relative symplastic water content at incipient plasmolysis (SWC_{IP}) is a measure of water volume within intracellular spaces as plasma membranes begin to withdraw from cell walls and turgor is lost inside the cell. Low relative symplastic water volume at incipient plasmolysis suggests cell walls are more flexible, meaning cells of this tissue could lose more water before plasma membranes retreat from cell walls, thus allowing for this immature or actively growing tissue to

maintain turgor for a longer period of time (Nobel, 2009). Values ranging from 0.17 to 0.22 have been measured in leaves and shoots of *Q. alba* (Parker and Pallardy, 1987), and values of 0.141, 0.208, 0.186, 0.238, and 0.156 for *Q. robur*, *Q. petraea*, *Q. pubescens*, mature *Q. ilex* shoots, and in immature *Q. ilex* shoots, respectively (Dreyer et al., 1990). Corcuera et al. (2002) also calculated higher values of 0.92, 0.85, and 0.73 SWC_{IP} for mature shoots of *Q. petraea*, *Q. pyrenaica*, and *Q. cerris*, respectively.

Osmotic potential at incipient plasmolysis ($\Psi\pi_{IP}$) is also determined from P-V curves. This is a measure of solute concentrations in cells (Nobel, 2009). Osmotic adjustment of water stressed plants is a way to maintain turgor at lower water potentials (Kramer and Boyer, 1995). Measurements of -1.37 and -1.84 MPa have been observed in expanding and mature leaf tissue of 'Colt' cherry (Ranney et al., 1991). Similar values were also measured in leaves and shoots of *Q. alba* seedlings (-1.62 to -1.77 MPa) (Parker and Pallardy, 1987), leaves of *J. nigra* seedlings (-1.42 to -1.58 MPa) (Parker and Pallardy, 1985), and in terminal shoots of *U. parvifolia* (-1.30 MPa) (Ranney et al., 1990). Maximum turgor pressure (P_{max}) within cells is collected from P-V curves as well. Beeson and Gilman (1992) quantified turgor pressures of 2.5 MPa for *Quercus virginiana*.

Bulk modulus of elasticity (E_o) estimates cell wall rigidity in plant samples. Low bulk modulus of elasticity indicates flexibility of cell walls, which aids in the ability of immature tissue being able to elongate and grow. Ranney et al. (1991) reported E_o values of 7.92 MPa for expanding leaves and 10.23 MPa for mature leaves of 'Colt' cherry. Values ranging from 3.61 to 8.73 MPa have been reported for leaves and shoots of *Q. alba* (Parker and Pallardy, 1987) and 9.15 MPa for shoots of *U. parvifolia*

(Ranney et al., 1990). Maximum modulus of elasticity (E_{max}) measurement is similar to the bulk modulus elasticity and is a measure of the rigidity of the plant tissue (Nobel, 2009). Parker and Pallardy (1985) reported values of 2.45 to 11.71 MPa for leaves of *J. nigra*.

Porometers and Infrared Gas Analyzers

Stomatal conductance is quantified using a porometer. Portable steady-state porometer systems compute g_s by measuring the flux in water vapor through leaf stomatal pores. Photosynthesis is measured using portable gas exchange systems such an infrared gas analyzer. Infrared gas analyzers (IRGA) measure concentrations of specific gases such as carbon dioxide and water vapor in air sample. Machines determine concentrations or concentration differences by measuring amounts of absorption occurring as an infrared laser is emitted through samples. Systems typically have two IRGA cells (*i.e.,* a reference and a measuring cell). A beam of infrared light is emitted at one end of the device. As it passes through, gases in the chambers absorb the radiation and the remaining unabsorbed laser quantity is measured. Internal calculations determine the difference between the emitted radiation and the amount of radiation not absorbed (Burough, 1980).

Plants of Study

Quercus virginiana

Quercus virginiana Mill., live oak or evergreen oak, is a member of the Fagaceae, beech and oak family (Smith, 1977). *Quercus* is Latin for oak and *virginiana* refers to Virginia, where this species is native (Watkins et al., 2005). *Q. virginiana* is widely distributed along warmer coastal regions of North America with a native range restricted to the Atlantic coast from southeastern Virginia to Florida and along the Gulf

Coast from Florida to Texas. *Q*. *virginiana* is found in diverse habitats, but usually grows in well-drained sandy coastal areas (Cullina, 2002). It is found throughout Florida (zones 7-10), and is plentiful in hammocks, scrubland, and lake margins (Cullina, 2002; Taylor, 1988; Watkins et al., 2005). Known for its low-slung, horizontal branches festooned with Spanish moss and other bromeliads, *Q. virginiana* has evergreen leaves that persist throughout the year with flushes occurring from March to September in Florida and (Brockman, 2001; Taylor, 1988) (Figure 1-1).

Height is generally 40-80 feet, but a variety of different forms (*i.e*., shrubby or dwarfed to large and spreading) can persist depending on location (Brockman, 2001; Cullina, 2002). *Q. virginiana* is mainly propagated from seed (Watkins et al., 2005). It is considered to be a fast growing species when young and under optimal growing conditions (Maccubbin and Tasker, 1997). This species is highly drought tolerant and has potential to root deeply, with the latter being an important trait for trees native to United States regions prone to hurricanes (Watkins et al., 2005).

In the 1800s and 1900s, the durable wood of *Q. virginiana* was used in ship building (Maccubbin and Tasker, 1997). Presently *Q. virginiana* is a popular ornamental landscape trees in Florida residential areas and along roadsides because of the drought tolerant nature and shade produced from the low, wide crown (Maccubbin and Tasker, 1997; Taylor, 1988; Watkins et al., 2005).

Ulmus parvifolia

Ulmus parvifolia Jacq., Chinese elm or lacebark elm, is a member of Ulmacea, elm family (Smith, 1977). *Ulmus* is Latin for elm and parvifolia refers to the small leaves (Watkins et al., 2005). *U. parvifolia* is native to the Orient (Brockman, 2001; Watkins et al., 2005). *U. parvifolia* is distributed throughout the southern and central United States

and along Atlantic, Gulf, and Pacific coasts. It is planted throughout Florida (zones 6-9), but grows best in northern and central Florida on well-drained soils (Taylor, 1988; Watkins et al., 2005). This species is known for having intricately patterned, exfoliating bark and a weeping growth habit with semi-evergreen leaves that typically flush from mid-March to August in Florida (Brockman, 2001; Watkins et al., 2005) (Figure 1-2).

Height is generally 20-60 feet (Brockman, 2001). *U. parvifolia* is propagated by seed and from cuttings (Watkins et al., 2005). 'Allée'® cultivars were released in the late 1990s. Cultivars were cloned from a tree located on the University of Georgia campus in Athens (More and White, 2002). Chinese elm is considered to be a fast growing species when young and under optimal growing conditions and can grow up to 3 feet per year (Taylor, 1988) (Figure 1-2). *U. parvifolia* has a high drought tolerance and appears to have a relatively shallow root system (Watkins et al., 2005).

The 'Allée'® cultivar is a common landscape tree in Florida. It is planted in buffer strips around parking lots and in highway medians due to this species tolerance of drought (Watkins et al., 2005). In the future Chinese elm might be used to combat Dutch elm disease due to resistance and given that it will hybridize with American elm species (More and White, 2002).

Figure 1-1. Photographs of *Quercus virginiana* taken in April 2011 at the Mid-Florida Research and Education Center in Apopka, Florida. A) Mature tree. B) Mature leaves. Photos are courtesy of Emily Massey.

Figure 1-2. Photographs of *Ulmus parvifolia* taken in April 2011 at the Mid-Florida Research and Education Center in Apopka, Florida. A) Mature tree. B) Colorful trunk bark. Photos are courtesy of Emily Massey.

CHAPTER 2
MATERIALS AND METHODS

Season One

In May 2010 2.5 year old seedlings of *Quercus virginiana* Mill. (live oak) and *Ulmus parvifolia* 'Allée'® Jacq. (Chinese elm) were obtained from Cherry Lake Tree Farm in Groveland, Florida. Trees were transplanted from #3 air-based root pruning containers to #7 black polyethylene containers (Nursery Supply, Co., Inc., Spartanburg, SC) using a substrate mixture of 60:40:10 (pine bark:Nupeat:coarse sand; Florida Potting Soil, Apopka, FL) with 2.9 kg of dolomite limestone and 0.86 kg of micronutrients per m^3 (Micro-Max, Scotts® Miracle-Gro® Co., Marysville, OH). The sand component does not contribute to the final bulk volume. NuPeat is a mixture of ⅓ Florida sedge peat, ⅓ composted hardwood bark, and ⅓ composted yard waste passed through a 12.5 mm screen. Trees were grown in full sun at the Mid-Florida Research and Education Center in Apopka, FL and micro-irrigated 3 times per day with two individual spray stakes per container (blue nursery pot stakes, 0.66 Lpm at 133 kPa, Maxijet Inc., Dundee, FL). In January 2011, remaining trees were transplanted into #10 black polyethylene containers (Nursery Supply, Co., Inc.) using the same substrate blend (Florida Potting Soil). Trees were fertilized throughout both seasons of data collection (Table 2-1).

Data were collected during periods of shoot elongation. In the summer of 2010, data collection began in early June. Six trees of each species were housed in an open-side gutter-connected sawtooth style greenhouse (18.5 x 24.6m) aligned east x west (Figure 2-1). Trees were randomly arranged in two rows aligned north x south with three control trees and three lysimeter trees of each species within each row. Control

trees were placed in wire basket stands above ground (Figure 2-2). Lysimeter trees were individually placed in suspension weighing lysimeters to monitor actual evapotranspiration (ET_A) and for individual irrigation control (Figure 2-3). A lysimeter consisted of a S-shaped aluminum mini-load cell (SSM-100, Interface Force, Inc., Scottsdale, AZ) suspended from a tripod support structure. A tree was suspended from a load cell by three chains that extended to a basket within a dry well placed in the ground such that the top of a container was about ground level (Beeson, 2011). Lysimeter data was collected and irrigation of lysimeters controlled with a data logger (CR10X, Campbell® Scientific, Inc., Logan, UT) attached to a multiplexer (AM 16-32, Campbell® Scientific, Inc., Logan, UT) and a control port module (SDM-CD16AC, Campbell® Scientific, Inc., Logan, UT). Mass of each tree was recorded every half hr. At midnight ET_A of each tree was calculated by subtracting mass at midnight from that recorded at 0500 hr EST (Eastern Standard Time). Irrigation volume was 125% ET_A, which was applied in three sub-volumes (midnight, 0100, and 0200 hr EST).

Irrigation of control trees was managed by a Sterling time clock (Superior Control Co., Inc., Valencia, CA) with one solenoid valve controlling irrigation for both species. Irrigation was applied at 1030, 1500, 2100 hr EST daily using two blue pot stakes (Maxijet Inc., Dundee, FL) per tree. Irrigation was applied for 5 minutes each cycle to insure thorough re-wetting of substrate. These trees will hereafter be referred to as frequently irrigated (FI).

After data was collected under well-watered conditions, a drought irrigation regime was imposed on lysimeter trees such that trees were slowly water stressed (~25 July 2010 and 30 July 2010 for live oak and Chinese elm, respectively). Drought stress was

initiated by applying nightly irrigation equivalent to 90% of daily ET_A in three sub-volumes as described previously. When daily ET_A had declined to about 90% of the well-irrigated rate, nightly irrigation was increased to 105% of daily ET_A to maintain the water stress level. Hereafter, well-watered lysimeter trees will be referred to as once-daily well-irrigation lysimeter (LDI) and water-stressed lysimeter trees will be referred to as water limited lysimeter irrigation (LLI).

Shoot Growth Measurements

Six elongating branches were selected on each tree. Branches were selected throughout a canopy. Lengths (millimeters) of elongating branches were measured at dawn (~0530 hr EST) and dusk (~1930 hr EST) using a CD-6" CS Absolute Digimatic caliper (Mitutoyo Corp., Japan). Elongation was recorded for five days and growth rates (mm/hr^{-1}) were calculated for day and nighttime measurements. Initial data was collected on FI and LDI trees. After water stress had been imposed and stabilized, shoot elongation measurements were collected for an additional five days at dusk and dawn for the same six branches on LLI trees.

Xylem Water Potential Measurements

Diurnal xylem water potential (Ψ_x) was measured during four collections of shoot elongation measurements. Measurements were recorded every two hrs from pre-dawn (~0500 hr EST) to post-dusk (~2100 hr EST) weather permitting, and collected from FI and LDI trees only. Measurements were concluded ~1900 hr EST when evening weather was cloudy or rainy. Measurements were made on individual, mature stems (≥11 cm in length) using a pressure chamber (Plant Moisture Status Console, Soilmoisture Equipment Corp., Santa Barbara, CA). Shoots were selected throughout a canopy. Shoots to be measured were covered with plastic wrap and aluminum foil one

hr prior to collection to minimize transpiration and allow stem Ψ_w to equilibrate with Ψ_x (Begg and Turner, 1970). Covered stems were removed from a branch with sharp shears (FELCO 2 Green™, Felco© SA Corp., Les Geneveys-sur-Coffrane, Switzerland) and enclosed in the pressure chamber within 45 seconds. Pressure was increased at a rate of 25 kPa s^{-1} using compressed nitrogen until water was just visible at the cut end.

Pressure-Volume Curves

Three to four mature individual shoots (~11 cm long) were collected for construction of pressure-volume (P-V) shortly after bud break for each tree. Bud break occurred in recurrent flushes from around March through September for both species. Pressure-volume curves were constructed just prior to shoot elongation measurements for well-watered trees. Mature tissue was tissue with fully expanded leaves and a stem that appeared to be lignified throughout (Figure 2-4 and Figure 2-5). Morning samples were taken throughout the canopy. Ends of stems were re-cut under water and placed in a 200mL beaker so that freshly cut ends were submerged in water. Plastic bags were secured over the tops of beakers and tissues were placed at ~3^{o}C for >24-hrs to re-saturate tissues and minimize transpiration (Ranney et al., 1990; Turner, 1988). Water potential was measured as described above (Figure 2-6). Volume of water loss was determined prior to pressurization by weighing each sample using an analytical balance (Mettler AE100, Mettler-Toledo®, Inc., Columbus, OH). Samples transpired freely on laboratory benches between Ψ_w measurements. Pressure-volume curves were constructed using Microsoft® Excel 2010 (Microsoft® Corp., Redmond, WA) and calculations were made as described previously (Meier et al., 1992; Tyree and Hammel, 1972; Urban et al., 1993).

Similar technique was followed for immature tissue with P-V curves constructed in the same manner. Immature growth was collected when new shoots had reached ~10 cm. Immature tissue had fully expanded leaves and a fairly flexible stem throughout (Figure 2-4 and 5). Lignified tissue (~2 cm) was needed on the proximal end of the stem for proper insertion into the pressure chamber.

Relation of Turgor Pressure to Shoot Growth

Turgor pressures (Ψ_p) were calculated for each diurnal Ψ_x measurement for each tree based on mean values from constructed P-V curves for that tree (Fig. 2-6). Calculated Ψ_p were plotted against corresponding balance pressures for each tree with mature and immature growth data analyzed separately. Equations were calculated using linear regression for each tree and age of tissue.

Diurnal Ψ_p were calculated using the diurnal Ψ_x measurements and corresponding regression equations. When calculating Ψ_p for some Ψ_x values, negative Ψ_p resulted. These values were recorded as zero. All positive Ψ_p values calculated were not altered. Daytime (~0500 to ~1900 hr EST) and nighttime (~1900 to ~0500 hr EST) diurnal Ψ_p were integrated over time (MPa-hr) for each tree. Measurement collection never extended past 2030 EST. Instead midnight measurements were based on Ψ_x of the following morning prior to sunrise. Integrated values were divided into respective growth measurements to calculate pressure-normalized growth rates (mm MPa-hr^{-1}) (Anselmi et al., 2004). Turgor pressure-normalized ($\Psi_{P\text{-}Norm}$) growth rates were calculated for measurements recorded on trees under well-watered conditions only. All calculations were made and the graphs were constructed using Microsoft® Excel 2010 (Microsoft® Corp., Redmond, WA).

Leaf Gas Exchange Measurements

Transpiration rate (E; mmol $m^{-2}s^{-1}$), and net photosynthesis (A; µmol $m^{-2}s^{-1}$) were measured using an ADC LC4 LC*i* portable gas exchange system (BioScientific® Ltd., Mountain View, CA). Calibration of the system occurred two years prior. Measurements were only collected from FI and LDI trees. Measurements were made at 0900, 1130, 1415, 1630, and 1900 hr EST on sunny days. Data collection for trees were on the 7 July 2010 (LDI elms), 24 June 2010 (FI elms), 7 July 2010 (LDI oaks), and 26 July 2010 (FI oaks). Samples were collected from the entire canopy. Leaves were fully expanded, mature, and located in full sun. These measurements were integrated over time to estimate a daily transpiration and net photosynthesis for each tree (Myers, 1988).

Stomatal conductance (g_s; mmol $m^{-2}s^{-1}$), and light levels (hυ; µmol $m^{-2}s^{-1}$) were measured using a *Li*-1600 portable steady state porometer (L*i*-Cor® Inc., Lincoln, NE). Initial measurements were collected from FI and LDI trees with subsequent measurements collected for LLI after trees were placed under water stress (~25 July 2010 and 30 July 2010 for live oak and Chinese elm, respectively). Measurements were made between ~1200 and ~1300 EST on sunny days. Data collection for trees were on the 8 July 2010 (LDI oaks), 26 July (FI oaks and LLI oaks), 31 July 2010 (LDI elms), and 2 August 2010 (FI elms and LLI elms). Leaves were fully expanded, mature, and located in full sun throughout the tree canopy.

Season Two

In 2011 new trees in #10 containers were randomly arranged in the same experimental system described above. FI trees were subjected to the same protocol described in Season One. Lysimeter trees were initially irrigated using a different well-

watered regime from that of 2010. Under this new regime, ~50% of ET_A occurring before solar noon (1300 hr EST) was applied individually for each lysimeter tree. At midnight (EST), daily ET_A was calculated for each tree as the difference in mass between 0600 hr and midnight EST plus the volume of the irrigation applied at solar noon. Night irrigation was calculated by multiplying daily ET_A by 1.3, then dividing by 2, with half applied at midnight and the other half applied at 0015 hr (Exp. 1). Hereafter, well-watered lysimeter trees from Season 2 will be referred to as twice-daily well-irrigation lysimeter ($LDI_{2\text{-}Daily}$).

After data collection under the well-watered regime, two additional irrigation regimes were imposed on lysimeter trees (Exp. 2) to manipulate turgor pressure over a 24-hr period. In the minimum night regime (Min-night), daily ET_A was calculated 0.5 hr after sunset (1945 hr EST) by subtracting the maximum mass recorded at 2030 hr EST the night before, by that measured at 1945 hr EST. Irrigation volume was 130% daily ET_A, with half applied at 1945 hr EST and the other half at 2000 hr EST. Maximum mass was determined after 30 minutes of drainage at 2030 hr EST. The Min-night regime was implemented to maximize turgor pressure over the night and minimize turgor pressure over the day. The second additional regime was a maximum night regime (Max-night). Here daily ET_A was calculated at sunrise (0630 hr EST) by subtracting the maximum mass recorded at 0715 hr EST the morning before, by that measured at 0630 hr EST. Irrigation volume was 130% daily ET_A, with half applied at 0630 hr EST and the other half at 0645 hr EST. Maximum mass was determined after 30 minutes of drainage. The Max-night regime was implemented to maximize turgor pressure over the day and minimize turgor pressure over the night. There was a one

day interval between one regime to the next. Overall protocol for Season Two was similar to Season One, except gas exchange measurements which were not collected during Season Two due to equipment malfunction.

Shoot Growth Measurements

Usually five elongating branches were selected on each tree for growth measurements for all irrigation regimes. For some trees, a maximum of three elongating branches were available. Branches were selected throughout a canopy and measurements were collected by sunrise (~0625 hr EST) and by sunset (~2000 hr EST) for three days in concurrence with diurnal water potential measurements. Shoot elongation measurements began one day after changing irrigation regimes.

Xylem Water Potential Measurements

Diurnal Ψ_x were measured during collection of shoot elongation measurements as described during Season One. Measurements were made for three days for each irrigation regime (FI, $LDI_{2\text{-Daily}}$, Max-night, and Min-night). Measurements were taken approximately every two hrs from pre-dawn (~0600 hr EST) to post-dusk (~2045 hr EST) weather permitting. Measurements were made on individual, mature shoots (≥11 cm in length) using a pressure chamber.

Pressure-Volume Curves

Three to four immature shoots (~11 cm long) were collected for construction of P-V curves after bud break for all trees as described in Season One. Pressure-volume curve measurements were made on three immature shoots for $LDI_{2\text{-Daily}}$ and FI trees prior the collection of diurnal Ψ_w measurements. Single replication curves were constructed for mature tissue for each $LDI_{2\text{-Daily}}$ tree post-implementation of irrigation regimes. Curves were constructed following the same protocol as outlined in data

collection during Season One. Pressure-volume curves were constructed shortly after budbreak for all trees. Curves were constructed prior to shoot elongation measurements for well-watered trees.

Relation of Turgor Pressure to Shoot Growth

Turgor pressure was related to growth using the same protocol described in Season One. Growth measurements and their concurrent diurnal Ψ_w measurements were collected for three days for each regime. Given the nature of the two irrigation regimes, graphs of Ψ_p and Ψ_w were constructed to determine if trends were apparent as expected. General trends were compared to trees under a well-watered condition ($LDI_{2\text{-}Daily}$) and similar trends were seen for FI trees (Figure 2-7 and Figure 2-8).

Statistical Analysis

Experimental design consisted of a complete randomized design with trees serving as replicates (N=3 per treatment) and measurements within individual trees serving as subreps. In Season One, growth elongation rate and pressure-normalized growth rates were analyzed as a 2 x 2 x 2 factorial, with two species, two irrigation regimes (FI vs LDI), and two time intervals (day vs night). Relative symplastic water content at incipient plasmolysis, osmotic potential at incipient plasmolysis, maximum turgor pressure, bulk modulus of elasticity, and maximum modulus of elasticity were also analyzed as a 2 x 2 x 2 factorial, with two species, two irrigation regimes (FI vs LDI), and two growth ages (mature growth vs immature growth). Stomatal conductance (g_s), light level, and leaf temperature measurements were analyzed as repeated measurements using a split plot design with tree water status (FI and LDI vs LLI) as the main plot and with two species and two irrigation regimes (well-watered vs water

stressed). Integrated measurements of photosynthesis (A) and transpiration (E) were analyzed as a 2 x 2 factorial, with two species and two irrigation regimes (FI vs LDI).

In Season 2, growth elongation rates and pressure-normalized growth rates under well-watered conditions were analyzed as a 2 x 2 factorial (FI and LDI, day and night growth rates) as repeated measures using a split plot design for Exp. 1. When comparing among irrigation regimes of lysimeter trees, data was analyzed independently by species (Exp. 2). Within a species, data was analyzed as a repeated measurements using a split plot design, with three irrigation regimes (control, Max-night, and Min-night), and two time intervals (day vs night), replicated three times.

Data was subjected to an analysis of variance and means separation between variables was obtained where appropriate using Fisher's Protected Least Significant Difference (LSD). All data was analyzed using SAS (9.2 SAS Institute Inc., Cary, NC).

Table 2-1. Tree fertilization schedule across Seasons One and Two.

Date (day, month, year)	Type	Amount (g)
20 May 2010	16-04-08[z]	9.5475
14 June 2010	16-04-08	9.5475
9 August 2010	16-04-08	7.5565
14 September 2010	16-04-08	7.5565
12 October 2010	14-14-14[y]	6.9401
2 February 2011	16-04-08	7.5565
22 March 2011	16-04-08	7.5565
4 April 2011	16-04-08	7.5565
22 April 2011	16-04-08	7.5565
16 May 2011	16-04-08	7.5565

[z] (N:P:K) quick release fertilizer (Pro-Source One, WinField Solutions™, Inc., Elwood, IN).

[y] (N:P:K) control release fertilizer (Osmocote®, Scotts® Miracle-Gro® Co., Marysville, OH).

Figure 2-1. Open-side gutter-connected sawtooth style greenhouse located at the Mid-Florida Research and Education Center in Apopka, Florida. Study trees were housed inside throughout Seasons One and Two of data collection. Photo is courtesy of Emily Massey.

Figure 2-2. Series of frequently irrigated trees (FI). A) *Quercus virginiana*. B) *Ulmus parvifolia*. Photos are courtesy of Emily Massey.

Figure 2-3. Series of lysimeter trees (LDI or $LDI_{2\text{-Daily}}$, or LLI). A) *Quercus virginiana*. B) *Ulmus parvifolia*. Photos are courtesy of Emily Massey.

Figure 2-4. Shoot age distinction of study trees for *Ulmus parvifolia*. A) Mature shoot. B) Immature shoot. Photos are courtesy of Emily Massey.

Figure 2-5. Shoot age distinction of study trees for *Quercus virginiana*. A) Mature shoot. B) Immature shoot. Photos are courtesy of Emily Massey.

Figure 2-6. Laboratory pressure-volume (P-V) curve station located at the Mid-Florida Research and Education Center in Apopka, Florida. Station includes an orange tank of compressed nitrogen, a pressure chamber (Plant Moisture Status Console, Soilmoisture Equipment Corp., Santa Barbara, CA), and an analytical balance (Mettler AE100, Mettler-Toledo®, Inc., Columbus, OH). Photo is courtesy of Emily Massey.

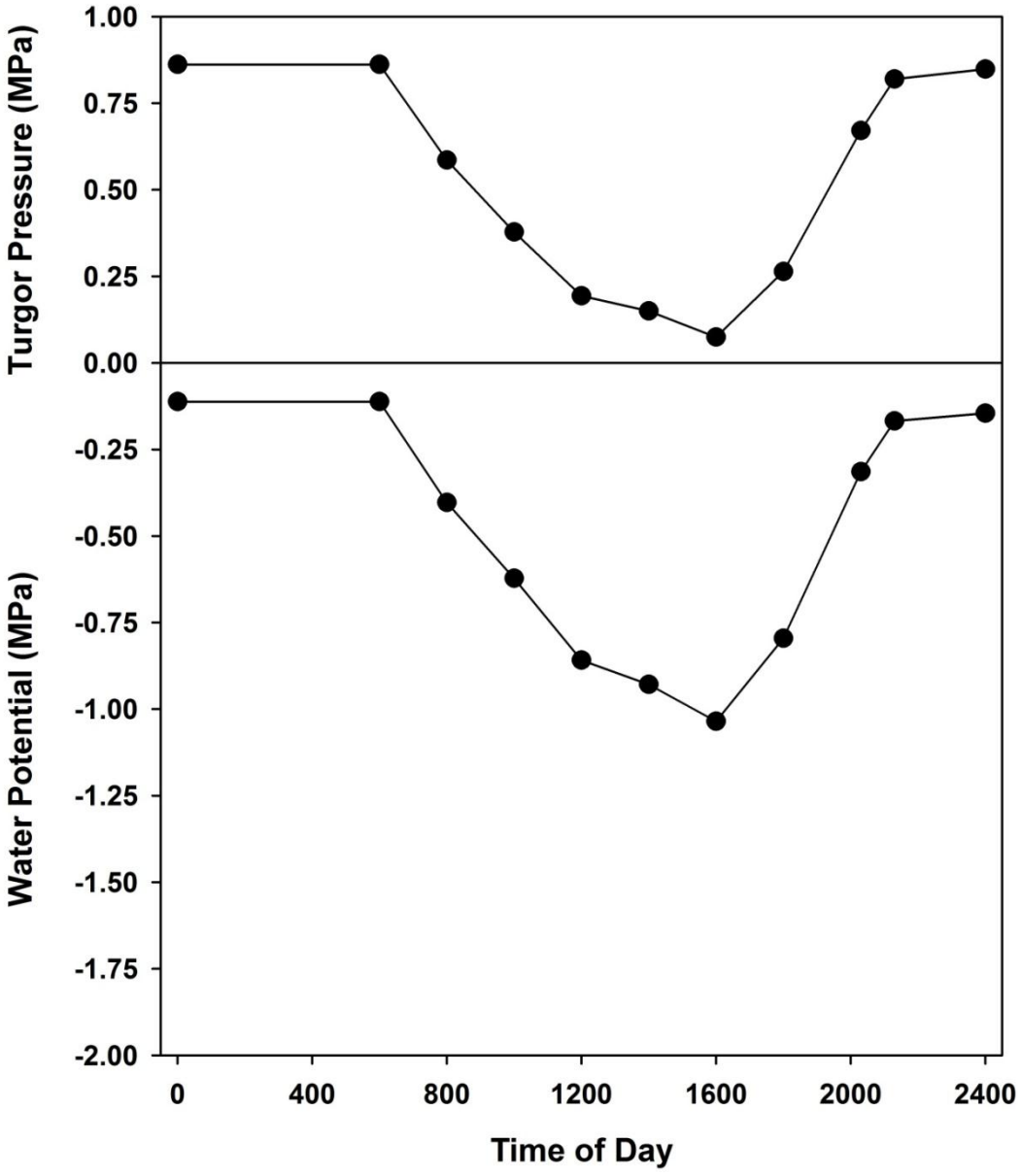

Figure 2-7. Diurnal water potential (Ψ_x) and subsequently estimated turgor pressure (Ψ_p) of frequently irrigated (FI) live oak in Season Two. Values were averaged over replicates (N=3) and three days of measurement (N=3).

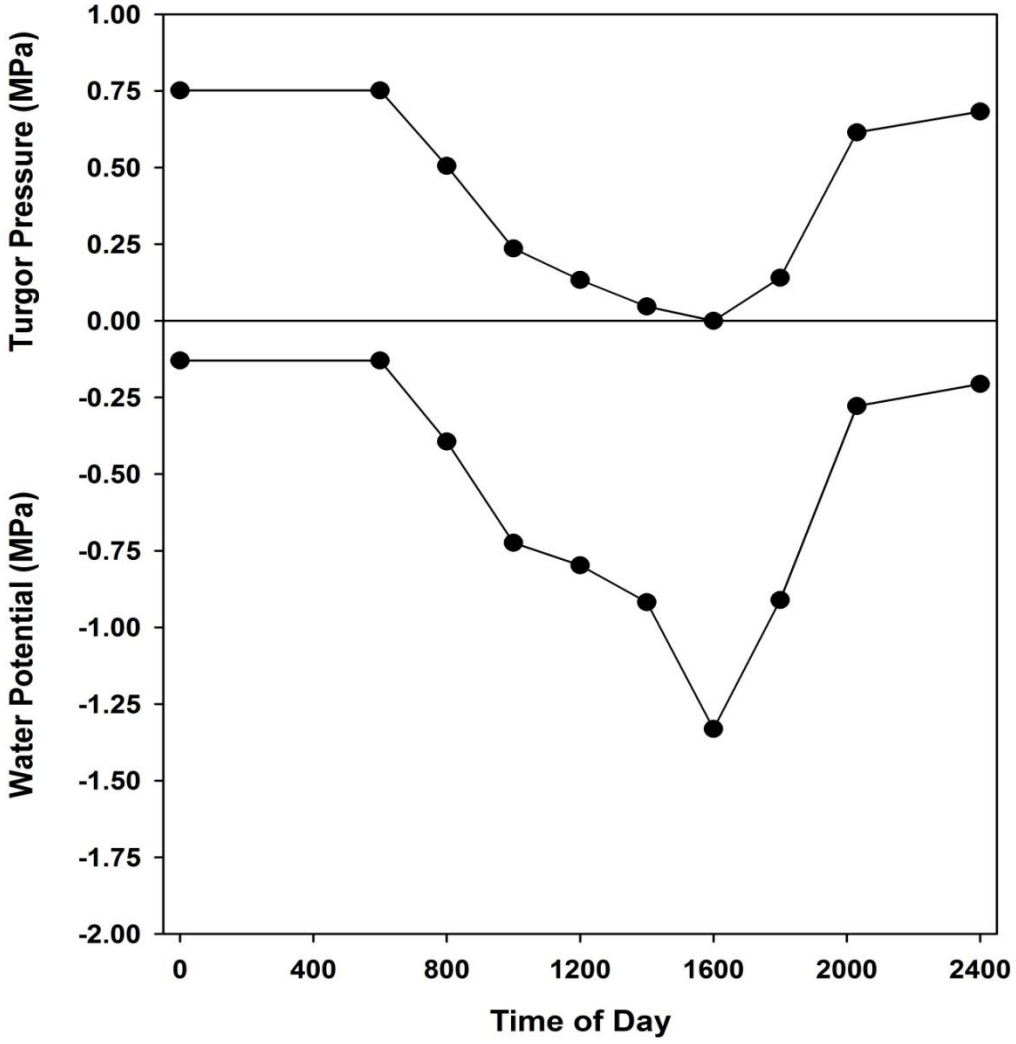

Figure 2-8. Diurnal water potential (Ψ_x) and subsequently estimated turgor pressure (Ψ_p) of frequently irrigated (FI) Chinese elm in Season Two. Values were averaged over replicates (N=3) and three days of measurement (N=3).

CHAPTER 3
RESULTS

Season One

Shoot Elongation Rate

Growth rates measured for a single day were concurrent with diurnal Ψ_w measurements. Measurements were recorded for frequently irrigated (FI) and once-daily well-irrigated lysimeter (LDI) trees. Shoot elongation rates were also analyzed over a two five day periods. Five day measurements were recorded for FI and LDI, then water limited lysimeter (LLI) trees.

Across the single day, shoots of Chinese elm (0.296 mm hr^{-1}) elongated at a greater rate than live oak shoots (0.208 mm hr^{-1}; P=0.043). Elongation rate was greater for FI trees (0.308 mm hr^{-1}) than LDI or LLI trees (0.213 mm hr^{-1}; P=0.016). Day and night elongation rates were similar within irrigation regimes.

Differences among irrigation regimes were further evident when measurements were compared across a five day period (Table 3-1). Shoots of FI trees elongated at greater rates than those of LDI and LLI, as seen in the single day comparison. Shoot elongation of LLI trees was slowest (P=0.002; Table 3-1). Differences between species were not significant. To gain greater insight, species were further analyzed separately. For live oak there were no differences among irrigation regimes. However, shoot elongation of Chinese elm was highly dependent on irrigation regime (P=0.036; Table 3-2). Elongation rate was 13 times greater for LDI trees than LLI trees, and 21 times greater for FI trees. Day and night elongation rates were not significantly different (P>0.05) within either species.

Relation of Turgor Pressure to Shoot Growth

Turgor pressure-normalized ($\Psi_{P\text{-}Norm}$) growth rates were calculated for each sample per tree to better ascertain the relationship between Ψ_p and shoot elongation. Calculations were made for shoots under FI and LDI conditions only. When species were analyzed together, there was a three-way interaction between species, irrigation regime and time of growth ($P \leq 0.0001$; Table 3-3). Overall daytime rates were higher than nighttime rates, with more variability associated with daytime rates. Daytime rates for live oak were similar across irrigation regimes, while Chinese elm daytime irrigation rates varied. While not significantly different, nighttime rates for Chinese elm varied 10-fold and LDI for live oak were double that of FI trees.

Pressure-Volume Curves

Pressure-volume curves were constructed from mature and immature shoots collected from well-watered trees (FI and LDI). Relative symplastic water content at incipient plasmolysis (SWC_{IP}) had a pair of two-way interactions between species and shoot age ($P=0.030$) and between irrigation regime and shoot age ($P= 0.007$). In the first interaction, mature shoots from both species and those of immature live oak had higher SWC_{IP} than immature Chinese elm shoots (Table 3-4). In the second interaction, shoots from LDI trees and mature tissue from FI trees had greater SWC_{IP} than immature shoots from FI trees (Table 3-5).

Osmotic potential at incipient plasmolysis ($\Psi\pi_{IP}$) also had two two-way interactions between species and shoot age ($P=0.001$) and irrigation regime and shoot age ($P \leq 0.0001$). In the first interaction, Chinese elm shoots and mature live oak shoots had a more negative $\Psi\pi_{IP}$ than immature live oak shoots (Table 3-6). In the second

interaction, shoots from FI trees and mature shoots of LDI trees were more negative when compared to immature tissue from LDI trees (Table 3-7).

There was a three-way interaction between species, irrigation regime, and shoot age for maximum turgor pressure (P_{max}; *P*= 0.004). Here mature shoots had a higher P_{max} than immature shoots (Table 3-8). Mature shoots P_{max} were double those and less variable than immature shoots. Mature shoots of Chinese elm had similar P_{max} values. Immature FI Chinese elm P_{max} values were similar to immature FI live oak.

Mature shoots (10.866 MPa) had a greater bulk modulus of elasticity (E_o) compared to immature shoots (3.270 MPa; *P*≤0.0001). Shoots from LDI trees (7.325 MPa) also had a larger E_o than shoots from FI trees (6.463 MPa; *P*=0.0001). For live oak, mature shoot E_o (11.308 MPa) was greater than that of immature shoots (3.612 MPa; *P*≤0.0001). Bulk modulus of elasticity for LDI trees (8.116 MPa) was also greater than FI trees (7.143 MPa; *P*=0.015). For Chinese elm there was a two-way interaction between irrigation regime and shoot age (*P*=0.041; Table 3-9). As in the oaks, mature shoot E_o was greater than that of immature shoots; however E_o of mature shoots from LDI trees was also greater than mature shoots from FI trees.

A two-way interaction also occurred between species and shoot age for maximum modulus of elasticity (E_{max}) (*P*=0.007; Table 3-10). Mature shoots had a larger value for E_{max} when compared to immature shoots, with mature live oak shoots being larger than mature Chinese elm shoots (Table 3-10).

Leaf Gas Exchange

Stomatal conductance (g_s) was measured for all irrigation regimes. Well-watered trees (FI and LDI) had a significantly higher mean g_s (225 mmol m^{-2} s^{-1}) than those under a water deficit (150 mmol m^{-2} s^{-1}; LLI) (*P*= 0.001). However, net photosynthesis

and transpiration rates were not significantly different. Light levels within the greenhouse were not different.

Season Two

Shoot Elongation Rate

In Experiment 1 (Exp. 1), shoot elongation rates were measured over a period of five continuous days. To ensure a well-watered condition, initial growth measurements were recorded on frequently irrigated (FI) and twice-daily well-irrigated lysimeter ($LDI_{2\text{-}Daily}$) trees for a five day period. There was a three-way interaction between species, irrigation regime, and time of growth for shoot elongation rates collected over a five day period (P=0.032; Table 3-11). Shoots of FI Chinese elm elongated at the highest rate. Rates of shoot elongation in $LDI_{2\text{-}Daily}$ live oak trees also exhibited high rates. Elongation rates for remaining trees were similar (Table 3-11). Notable for each species and irrigation regime combination, shoot elongation rates were the same between day and night except for the $LDI_{2\text{-}Daily}$ Chinese elm.

In Experiment 2 (Exp. 2), growth measurements collected with diurnal Ψ_w measurements occurred across three different irrigation regimes. Regimes consisted of trees which were $LDI_{2\text{-}Daily}$, minimum night irrigation (Min-night), and Maximum night irrigation (Max-night). Min-night trees were irrigated shortly after sunset. Max-night trees were irrigated shortly after dawn. Irrigation volumes were calculated by measuring actual evapotranspiration rates (ET_A) daily. Species were analyzed separately.

There was a two-way interaction between irrigation regime and time of growth for live oak trees (P=0.0068). Shoot elongation was highest during Min-night at night and for $LDI_{2\text{-}Daily}$ trees at night. Shoot elongation was lowest for Max-night irrigation at night and for Min-night irrigation during the day (Table 3-12). Although shoot elongation rate

of Max-night during the day was 25% greater than that of Max-night at night, elongation rates were similar. The same two-way interaction also occurred in Chinese elm trees (P=0.044). Shoot elongation was the highest for $LDI_{2\text{-}Daily}$ trees during the night and shoot elongation was the lowest for trees irrigated under the Max-night regime during the night (Table 3-13).

Relation of Turgor Pressure to Shoot Growth

Turgor pressure-normalized ($\Psi_{P\text{-}Norm}$) growth rates were calculated using the elongation rates described above and followed the protocol outlined in Season One. New P-V curves were generated for immature growth prior to any alteration in irrigation regime and prior to diurnal Ψ_w measurements. A single P-V curve was made for all lysimeter trees after the last irrigation regime (Max-night) was implemented.

When analyzed across species there was a two-way interaction between species and time of growth (P=0.042). Turgor pressure-normalized growth rates were higher in Chinese elm than in live oak trees, with daytime Chinese elm rates being three and four times greater than live oak daytime and nighttime rates, respectively. Daytime rates were also greater than nighttime rates for both species with daytime ($\Psi_{P\text{-}Norm}$) growth rates double to those of nighttime rates in Chinese elm. Daytime live oak rates were higher, but not the same extent as Chinese elm rates (Table 3-14).

To better understand the relationship between turgor and shoot elongation, species were analyzed separately across irrigation regimes. Variation was found between treatments for live oak (P=0.010). Twice-daily well-irrigated lysimeter ($LDI_{2\text{-}Daily}$; 0.039 mm MPa-hr^{-1}) trees had greater $\Psi_{P\text{-}Norm}$ growth rates when compared to those of the Max-night irrigation (0.023 mm MPa-hr^{-1}) regime. The Min-night (0.031 mm MPa-hr^{-1}) regime produced intermediate $\Psi_{P\text{-}Norm}$ growth rates that were similar to the

other two. A two-way interaction between irrigation and time of growth occurred in Chinese elm (P=0.003). For Chinese elm, $LDI_{2\text{-Daily}}$ and Min-night trees had the greatest ($\Psi_{P\text{-Norm}}$) growth rates during the daytime, with rates three to four times greater than the lowest values. Rates for nighttime Max-night and Min-night were the lowest (Table 3-15).

Measured diurnal water potential (Ψ_x) and estimated turgor pressure (Ψ_p) used to calculate turgor pressure normalized ($\Psi_{P\text{-Norm}}$) growth rates were further investigated.

Diurnal water potential (Ψ_x) and calculated diurnal turgor pressure (Ψ_p) values were graphed (Figure 3-1 and Figure 3-2). Graphed patterns followed similar trends regardless of species. As typically reported, Ψ_x was generally constant over night from sunset to sunrise (Figure 3-1 and 3-2). During the day, Ψ_x declined after sunrise to reach a minimum after midday (~1400 to 1600 Eastern Standard Time; EST), later than normally reported for more northern latitudes (Abrams and Knapp, 1987). Thereafter, Ψ_x increased relatively quickly to achieve a minimum at sunset. This general trend was independent of irrigation regime. However, there were characteristics of each irrigation regime that influenced estimated Ψ_p. $LDI_{2\text{-Daily}}$ and Min-night irrigation had relatively high Ψ_p values and relatively less negative Ψ_x values at sunrise and sunset. Max-night irrigation had relatively lower Ψ_p and more negative Ψ_x values than those of the other two treatments at sunset. A small peak was visible ~0700 for Max-night irrigation for both the water potential and turgor pressure graph. This peak was not seen for the other two irrigation regimes. Around midday, turgor pressure for both species was zero with the duration of this loss of turgor longer for Chinese elm. Max-night and $LDI_{2\text{-Daily}}$ Ψ_x values were visibly less negative than those of Min-night irrigation. While data were

not analyzed statistically, Max-night values for both sunrise and sunset were more negative (Ψ_x) or less (Ψ_p) than those of Min-night and $LDI_{2\text{-Daily}}$, and values for the Min-night and $LDI_{2\text{-Daily}}$ appeared to be similar.

Pressure-Volume Curves

Pressure-volume curves were constructed following protocol as outlined in Season One, with an exception in the number of samples collected. Measurements were made on three immature shoots for $LDI_{2\text{-Daily}}$ and FI trees, with only one mature shoot measured for each $LDI_{2\text{-Daily}}$ tree. Mature shoots (0.632) had a higher SWC_{IP} than immature shoots (0.400; $P \leq 0.0001$).

There was a two-way interaction between species and shoot age for $\Psi\pi_{IP}$ (Table 3-16; $P=0.033$). Immature shoots and mature live oak shoots had a more negative $\Psi\pi_{IP}$ than mature Chinese elm shoots.

A two-way interaction between species and shoot age also was measured for maximum turgor pressure (P_{max}) ($P=0.048$). Larger P_{max} values were measured in mature shoots over immature shoots (Table 3-17).

Mature shoots (10.473 MPa) had a greater bulk modulus of elasticity (E_o) when compared against immature shoots (3.641 MPa; $P \leq 0.0001$). Values also varied between species, with a higher E_o for live oak shoots (4.975 MPa) when compared to Chinese elm (4.260 MPa; $P=0.0007$).

Live oak shoots (2.218 MPa) had a larger value for maximum modulus of elasticity (E_{max}) when compared to shoots of Chinese elm (1.817 MPa; $P=0.0022$). Maximum modulus of elasticity was also larger for mature shoots (3.453 MPa) when compared to immature shoots (1.778 MPa; $P \leq 0.0001$), and irrigation regimes varied, with E_{max} for $LDI_{2\text{-Daily}}$ trees (2.407 MPa) higher than FI trees (1.498 MPa; $P \leq 0.0001$).

Table 3-1. Shoot elongation rates measured across a five day period for frequently irrigated (FI), once-daily well-irrigation lysimeter (LDI), and once-daily limited irrigation (LLI) regimes across species.

Irrigation regime	Shoot elongation (mm hr^{-1})
FI[z]	0.330 a[y]
LDI	0.259 b
LLI	0.027 c

[z] Each mean represents N=270, 311, and 259 for FI, LDI, and LLI respectively.

[y] Mean separation by Fisher's Protected LSD. Means with same letter were not significantly different at $\alpha \leq 0.05$.

Table 3-2. Chinese elm shoot elongation rates measured across a five day period for frequently irrigated (FI), once-daily well-irrigation lysimeter (LDI), and once-daily limited irrigation (LLI) regimes.

Irrigation regime	Shoot elongation (mm hr^{-1})
FI[z]	0.409 a[y]
LDI	0.262 b
LLI	0.019 c

[z] Each mean represents N=162, 162, and 99 for FI, LDI, and LLI respectively.

[y] Mean separation by Fisher's Protected LSD. Means with same letter were not significantly different at $\alpha \leq 0.05$.

Table 3-3. Interaction between species, irrigation regime, and time of growth for turgor pressure-normalized ($\Psi_{P\text{-}Norm}$) growth rate over a single day for frequently irrigated (FI) and once-daily well-irrigation lysimeter (LDI) across species.

Species*irrigation regime*time of growth	$\Psi_{P\text{-}Norm}$ growth rate (mm MPa-hr^{-1})
Chinese elm*FI*day[z]	0.073 a[y]
live oak*LDI*day	0.046 b
live oak*FI*day	0.032 bc
Chinese elm*LDI*day	0.020 c
Chinese elm*FI*night	0.002 d
live oak*LDI*night	0.001 d
live oak*FI*night	0.0004 d
Chinese elm*LDI*night	0.0002 d

[z] Each mean represents N=18, 18, 12, 18, 18, 18, 12, and 18 for the combinations above in descending order.

[y] Mean separation by Fisher's Protected LSD. Means with same letter were not significantly different at $\alpha \leq 0.05$.

Table 3-4. Interaction of species and shoot age for relative symplastic water content at incipient plasmolysis (SWC_{IP}) during Season One across frequently irrigated (FI), and once-daily well irrigation regimes (LDI) across species.

Species*shoot age	SWC_{IP}
live oak*mature[z]	0.634 a[y]
Chinese elm*mature	0.592 a
live oak*immature	0.578 a
Chinese elm*immature	0.394 b

[z] Each mean represents N=19, 20, 17, and 19 for the combinations above in descending order.

[y] Mean separation by Fisher's Protected LSD. Means with same letter were not significantly different at α≤ 0.05.

Table 3-5. Interaction of irrigation regime and shoot age for relative symplastic water content at incipient plasmolysis (SWC_{IP}) during Season One across frequently irrigated (FI) and once-daily well-irrigation lysimeter (LDI) across species.

Irrigation regime*shoot age	SWC_{IP}
LDI*mature[z]	0.616 a[y]
LDI*immature	0.599 a
FI*mature	0.577 a
FI*immature	0.439 b

[z] Each mean represents N=18, 18, 16, and 23 for the combinations above in descending order.

[y] Mean separation by Fisher's Protected LSD. Means with same letter were not significantly different at α≤ 0.05.

Table 3-6. Interaction of species and shoot age for osmotic potential at incipient plasmolysis ($\Psi\pi_{IP}$) during Season One across frequently irrigated (FI) and once-daily well-irrigation lysimeter (LDI) across species.

Species*shoot age	$\Psi\pi_{IP}$ (MPa)
live oak*mature[z]	-2.594 a[y]
Chinese elm*immature	-2.494 a
Chinese elm*mature	-2.431 a
live oak*immature	-1.754 b

[z] Each mean represents N=18, 23, 18, and 16 for the combinations above in descending order.

[y] Mean separation by Fisher's Protected LSD. Means with same letter were not significantly different at α≤ 0.05.

Table 3-7. Interaction of irrigation regime and shoot age for osmotic potential at incipient plasmolysis ($\Psi\pi_{IP}$) during Season One across frequently irrigated (FI) and once-daily well-irrigation lysimeter (LDI) across species.

Irrigation regime*shoot age	$\Psi\pi_{IP}$ (MPa)
FI*immature[z]	-2.781 a[y]
LDI*mature	-2.583 ab
FI*mature	-2.434 b
LDI*immature	-1.630 c

[z] Each mean represents N=19, 19, 17, and 20 for the combinations above in descending order.

[y] Mean separation by Fisher's Protected LSD. Means with same letter were not significantly different at $\alpha \leq 0.05$.

Table 3-8. Interaction between species, irrigation regime, and shoot age for maximum turgor pressure (P_{max}) during Season One across frequently irrigated (FI) and once-daily well-irrigation lysimeter (LDI) across species.

Species*irrigation regime*shoot age	P_{max} (MPa)
live oak*FI*mature[z]	4.731 a[y]
Chinese elm*LDI*mature	4.104 b
live oak*LDI*mature	4.086 b
Chinese elm*FI*mature	3.800 b
Chinese elm*FI*immature	1.936 c
live oak*FI*immature	1.588 cd
Chinese elm*LDI*immature	1.367 d
live oak*LDI*immature	1.31 d

[z] Each mean represents N=8, 9, 10, 9, 12, 7, 11, and 9 for the combinations above in descending order.

[y] Mean separation by Fisher's Protected LSD. Means with same letter were not significantly different at $\alpha \leq 0.05$.

Table 3-9. Interaction of irrigation regime and shoot age for bulk modulus of elasticity of Chinese elm during Season One across frequently irrigated (FI) and once-daily well-irrigation lysimeter (LDI).

Irrigation regime*shoot age	E_o (MPa)
LDI*mature[z]	11.28 a[y]
FI*mature	9.782 b
FI*immature	3.124 c
LDI*immature	2.930 c

[z] Each mean represents N=18, 18, 12, and 11 for the combinations above in descending order.

[y] Mean separation by Fisher's Protected LSD. Means with same letter were not significantly different at α≤ 0.05.

Table 3-10. Interaction of species and shoot age for maximum modulus of elasticity (E_{max}) during Season One across frequently irrigated (FI) and once-daily well-irrigation lysimeter (LDI) across species.

Species*shoot age	E_{max} (MPa)
live oak*mature[z]	2.198 a[y]
Chinese elm*mature	1.610 b
live oak*immature	1.144 c
Chinese elm*immature	1.144 c

[z] Each mean represents N=18, 18, 16, and 23 for the combinations above in descending order.

[y] Mean separation by Fisher's Protected LSD. Means with same letter were not significantly different at α≤ 0.05.

Table 3-11. Interaction of species, irrigation regime, and time of growth for shoot elongation over a period of five days during Experiment 1 (Exp. 1) for Season Two. Measurements were collected from frequently irrigated (FI) and twice-daily well-irrigation lysimeter ($LDI_{2\text{-}Daily}$) across species.

Species*irrigation regime*time of growth	Shoot elongation (mm hr^{-1})
Chinese elm*FI*day[z]	0.352 a[y]
Chinese elm*FI*night	0.339 a
live oak* $LDI_{2\text{-}Daily}$*night	0.236 b
live oak* $LDI_{2\text{-}Daily}$*day	0.193 bc
live oak*FI*day	0.176 c
Chinese elm* $LDI_{2\text{-}Daily}$ *day	0.163 c
live oak*FI*night	0.148 c
Chinese elm* $LDI_{2\text{-}Daily}$ *night	0.108 d

[z] Each mean represents N=75, 60, 60, 75, 75, 75, 60, and 60 for the combinations above in descending order.

[y] Mean separation by Fisher's Protected LSD. Means with same letter were not significantly different at $\alpha \leq 0.05$.

Table 3-12. Interaction of irrigation regime and time of growth for shoot elongation in live oak over the course of diurnal Ψ_w measurements during Experiment 2 (Exp. 2) for Season Two.

Irrigation regime*time of growth	Shoot elongation (mm hr^{-1})
$LDI_{2\text{-}Daily}$ [z]*night[y]	0.252 a[x]
Min-night[w]*night	0.218 ab
Max-night[v]*day	0.195 ab
$LDI_{2\text{-}Daily}$ *day	0.169 b
Max-night*night	0.155 bc
Min-night*day	0.091 c

[z] Twice-daily well-irrigation lysimeter ($LDI_{2\text{-}Daily}$).

[y] Each mean represents N=43, 27, 27, 43, 27, and 27 for the combinations above in descending order.

[x] Mean separation by Fisher's Protected LSD. Means with same letter were not significantly different at $\alpha \leq 0.05$.

[w] Minimum night irrigation regime (Min-night)

[v] Maximum night irrigation regime (Max-night)

Table 3-13. Interaction of irrigation regime and time of growth for shoot elongation in Chinese elm over the course of diurnal Ψ_w measurements during Experiment 2 (Exp. 2) for Season Two.

Irrigation regime*time of growth	Shoot elongation (mm hr^{-1})
$LDI_{2\text{-}Daily}$ [z]*night[y]	0.320 a[x]
$LDI_{2\text{-}Daily}$ *day	0.279 ab
Min-night[w]*night	0.231 bc
Min-night*day	0.183 cd
Max-night[v]*day	0.140 de
Max-night*night	0.076 e

[z] Twice-daily well-irrigation lysimeter ($LDI_{2\text{-}Daily}$).

[y] Each mean represents N=43, 27, 27, 43, 27, and 27 for the combinations above in descending order.

[x] Mean separation by Fisher's Protected LSD. Means with same letter were not significantly different at $\alpha \leq 0.05$.

[w] Minimum night irrigation regime (Min-night)

[v] Maximum night irrigation regime (Max-night)

Table 3-14. Interaction between species and time of growth for turgor pressure-normalized ($\Psi_{P\text{-}Norm}$) growth rate over the course of diurnal Ψ_w measurements during Experiment 2 (Exp. 2) for Season Two across frequently irrigated (FI) and twice-daily well-irrigation lysimeter ($LDI_{2\text{-}Daily}$) across species.

Species*time of growth	$\Psi_{P\text{-}Norm}$ growth rate (mm MPa-hr^{-1})
Chinese elm*day[z]	0.107 a[y]
Chinese elm*night	0.055 b
live oak*day	0.0364 c
live oak*night	0.0267 d

[z] Each mean represents N=143, 143, 140, and 140 for the combinations above in descending order.

[y] Mean separation by Fisher's Protected LSD. Means with same letter were not significantly different at $\alpha \leq 0.05$.

Table 3-15. Interaction of irrigation regime and time of growth for turgor pressure-normalized ($\Psi_{P\text{-}Norm}$) growth rate in Chinese elm during Experiment 2 (Exp. 2) for Season Two for twice-daily lysimeter irrigation regimes ($LDI_{2\text{-}Daily}$), Minimum night regime (Min-night), and Maximum night regime (Max-night). Each mean represents N=36.

Irrigation regime*time of growth	$\Psi_{P\text{-}Norm}$ growth rate (mm MPa-hr^{-1})
$LDI_{2\text{-}Daily}$ *day	0.154 a[z]
Min-night*day	0.081 b
$LDI_{2\text{-}Daily}$ *night	0.065 c
Max-night*day	0.061 c
Max-night*night	0.039 d
Min-night*night	0.037 d

[z] Mean separation by Fisher's Protected LSD. Means with same letter were not significantly different at α≤ 0.05.

Table 3-16. Interaction of species and shoot age for osmotic potential at incipient plasmolysis ($\Psi\pi_{IP}$) during Season Two across species.

Species*shoot age	$\Psi\pi_{IP}$ (MPa)
Chinese elm*immature[z]	-2.495 a[y]
live oak*immature	-2.287 a
live oak*mature	-1.808 a
Chinese elm*mature	-1.179 b

[z] Each mean represents N=18, 18, 3, and 3 for the combinations above in descending order.

[y] Mean separation by Fisher's Protected LSD. Means with same letter were not significantly different at α≤ 0.05.

Table 3-17. Interaction of species and shoot age for maximum turgor pressure (P_{max}) during Season Two across species.

Species*shoot age	P_{max} (MPa)
Chinese elm*mature[z]	4.14 a[y]
live oak*mature	3.57 a
live oak*immature	2.19 b
Chinese elm*immature	2.13 b

[z] Each mean represents N=18, 18, 3, and 3 for the combinations above in descending order.

[y] Mean separation by Fisher's Protected LSD. Means with same letter were not significantly different at α≤ 0.05.

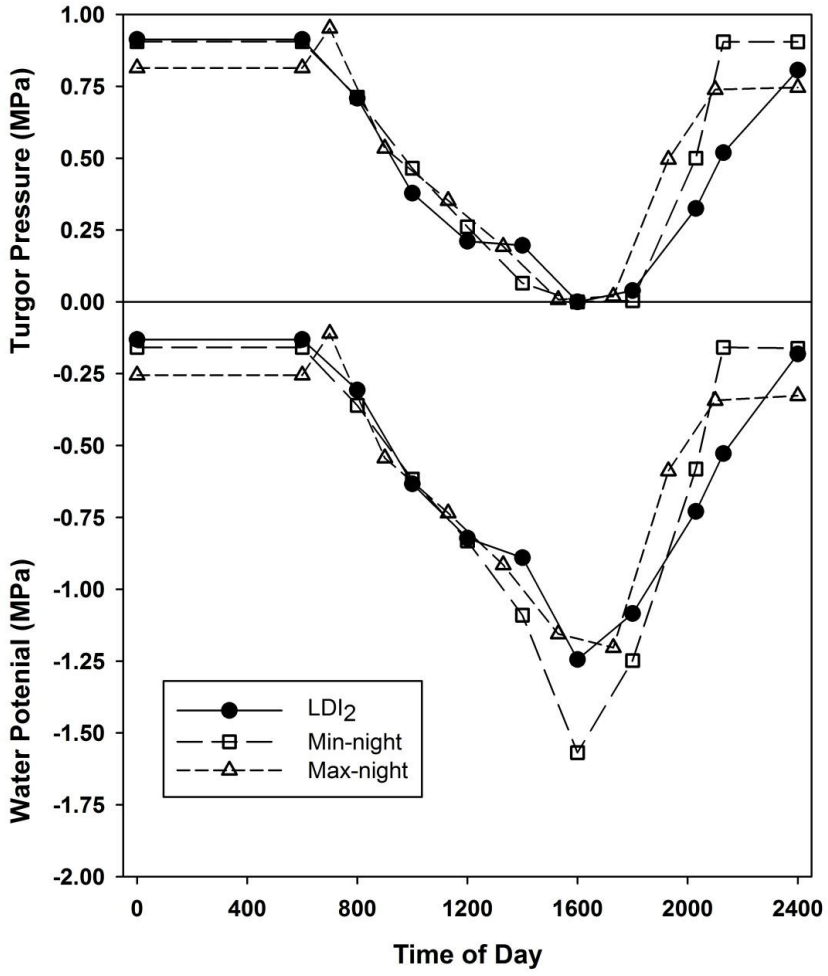

Figure 3-1. Diurnal water potential (Ψ_x) and subsequently estimated turgor pressure (Ψ_p) of live oak in Season Two. Values were averaged over replicates (N=3) and three days of measurement (N=3). Treatments include twice-daily well-watered lysimeter irrigation ($LDI_{2\text{-}Daily}$), minimum night irrigation (Min-night) and maximum night irrigation (Max-night).

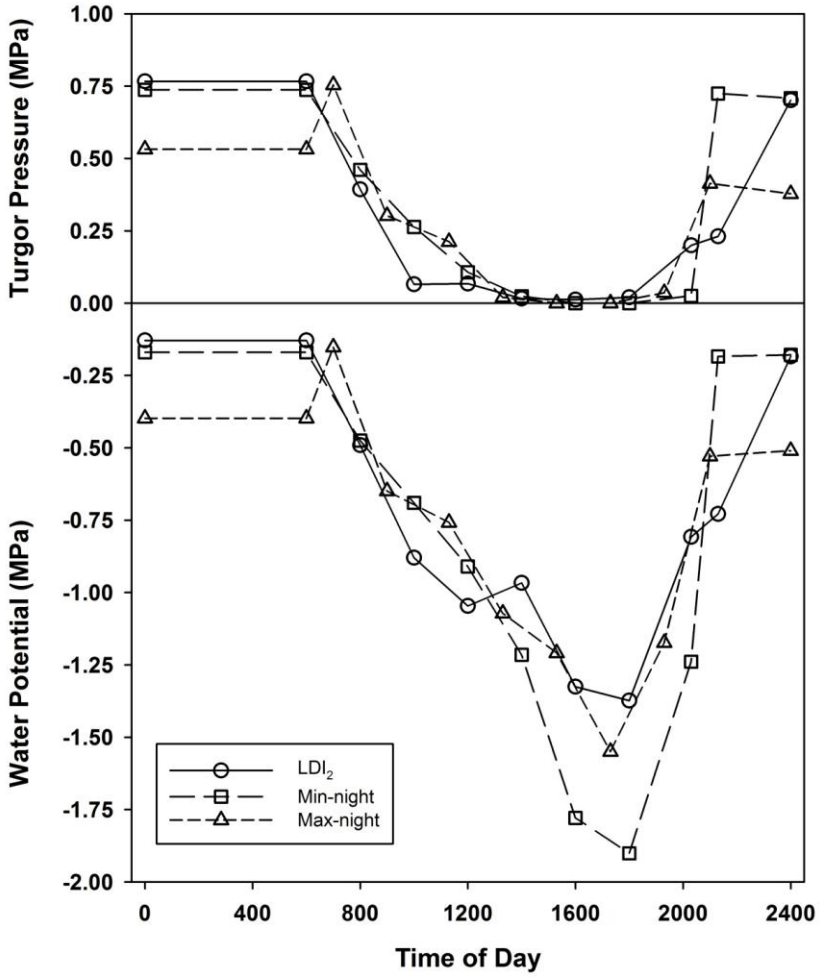

Figure 3-2. Diurnal water potential (Ψ_x) and subsequently estimated turgor pressure (Ψ_p) of Chinese elm in Season Two. Values were averaged over replicates (N=3) and three days of measurement (N=3). Treatments include twice-daily well-watered lysimeter irrigation ($LDI_{2\text{-}Daily}$), minimum night irrigation (Min-night) and maximum night irrigation (Max-night).

CHAPTER 4
DISCUSSION

Seasons One and Two

Measurements were collected for containerized *Quercus virginiana* and *Ulmus parvifolia* seedlings over two growing seasons. In 2010, data was collected from June through September, and in 2011 data was collected from March through June. All measurements were collected on actively growing trees, which were subjected to monitored irrigation regimes. Frequently irrigated (FI) trees were irrigated three times a day to container capacity. In Season One, lysimeter trees were irrigated once-daily (LDI) to ensure a well-irrigated condition. These trees were later irrigated at 90% ET_A in order to impose mild water stress (water limited lysimeter irrigation, LLI). In Season Two FI trees were watered following the same protocol outlined in Season One. Protocol was altered for well-watered lysimeter trees such that lysimeter trees were irrigated twice-daily (twice-daily well-irrigated lysimeter, $LDI_{2\text{-}Daily}$). Two additional regimes were included in which irrigation was applied once-daily. For trees irrigated under the minimum night regime (Min-night), irrigation was applied shortly after sunset. Post-sunset irrigation resulted in maximum Ψ_w and therefore minimum water stress throughout the night. For trees irrigated under the maximum night regime (Max-night), irrigation was applied shortly after dawn. Dawn irrigation resulted in sub-maximum Ψ_w during the night and therefore an elevated level of water stress.

Leaf Gas Exchange

Stomatal conductance (g_s) was collected within periods of shoot elongation during Season One for all trees around midday only. Higher mean g_s was measured in well-

watered trees of both species (225 mmol m^{-2} s^{-1}; FI and LDI) when compared to those under a water deficit (150 mmol m^{-2} s^{-1}; LI).

Overall, g_s for well-watered trees agreed with those of previously studied species. Gallego et al (1994) reported g_s around 150-200 mmol m^{-2} s^{-1} for *Quercus pyrenaica*. Lower g_s for water-stressed trees were also consistent with previously cited literature. Plants close stomata to minimize water loss during stress and maintain water status. Stomatal aperture is mediated, in part, by availability of moisture in soils (Lambers et al., 2008). Decreased g_s rates were measured in four drought stressed oleander clones (Niu et al., 2008). Gu et al. (2007) also demonstrated a strong relationship in the reduction of g_s and P_n rates in four birch genotypes under water deficit.

No differences were measured in light levels of the greenhouse. No differences were found for mean photosynthetic or transpiration rates between species or irrigation regimes. Mean photosynthetic rates of 22 and 21 µmol m^{-2} s^{-1} for live oak and Chinese elm, respectively, were similar to other woody species. Maximum photosynthetic rates were measured at ~22 µmol m^{-2} s^{-1} for *Picea abies* and ~16 µmol m^{-2} s^{-1} for *Quercus pubescens*, respectively (Haldimann et al., 2008; Maier-Maercker, 1998). While rates for three year old grafted and micropropagated *Ulmus glabra* were ~33 and 23 µmol m^{-2} s^{-1}, respectively (Durkovic et al., 2010).

These differences in g_s, yet similarities in leaf gas exchange, indicates that differences in growth rates and pressure-volume (P-V) curve parameters were more than likely due to changes in irrigation regime and not changes in photosynthetic rates. Furthermore, these results support that well-watered trees (FI and LDI) were

physiologically similar despite the differing amounts and number of irrigation cycles applied to them.

Pressure-Volume Curves

Overall, mature shoots in both seasons had a higher relative symplastic water volume at incipient plasmolysis (SWC_{IP}) than immature shoots, with mature shoot values ranging from (0.634-0.577; Table 3-4 and Table 3-5). In Season Two, there were no interactions with shoot age (0.632 and 0.400 for mature and immature shoots). However in Season One, effects of shoot age interacted with species and irrigation regime separately. Immature shoots of live oak (0.578) and LDI (0.599) trees had values similar to mature shoots (Table 3-4 and Table 3-5). High values measured in immature shoots of live oak indicate they are less plastic than immature shoots of Chinese elm. Limited interactions with shoot age in Season Two may have been the result of imbalance in shoot sample numbers due to only one shoot replication having been analyzed per $LDI_{2\text{-}Daily}$ tree, with no samples collected from FI trees. Alternatively, three immature shoot replications were collected for FI and $LDI_{2\text{-}Daily}$ trees.

Tissue collected was based on visual estimation of maturity and flexibility of tissue. High flexibility of shoots was attributed to little or no lignin in this tissue. Identification of mature and immature growth was easier for Chinese elm opposed to live oak. Immature shoots of Chinese elm were highly flexible with red coloration in the leaves (Figure 2-4 and Figure 2-5). While new flushes of live oak appeared more flexible than mature tissue, young live oak tissues were distinguished by pale green leaves and red-brown stems in contrast to dark green leaves and light brown stems in mature shoots (Figure 2-4 and Figure 2-5).

High SWC_{IP} is typically found in mature shoots; whereas lower values are often associated with immature, actively growing tissue due to the highly flexible cell walls (Nobel, 2009). As in this study, higher values were measured in mature shoots (0.238) when compared to immature shoots (0.156) from *Q. ilex* (Dreyer et al., 1990). Corcuera et al. (2002) also calculated similar SWC_{IP} values measured in study trees in mature shoots *Q. frainetto* and *Q. cerris* (0.73 and 0.72).

Differences in osmotic potential at incipient plasmolysis ($\Psi\pi_{IP}$) were variable between Seasons One and Two. There was a two-way interaction between species and shoot age for $\Psi\pi_{IP}$ in both seasons (Table 3-6 and Table 3-17). In Season One, mature shoots and immature Chinese elm shoots (-2.594 to -2.431 MPa) had a more negative $\Psi\pi_{IP}$ than immature live oak shots (-1.754 MPa; Table 3-6). In contrast the opposite was found in Season Two, where live oak shoots and immature Chinese elm shoots (-2.495 to -1.808 MPa) had a more negative $\Psi\pi_{IP}$ than mature Chinese elm shoots (-1.179 MPa; Table 3-17). In Season One there was also a two-way interaction between irrigation regime and shoot age (Table 3-7). Here shoots from FI trees (-2.781 to -2.434 MPa) and mature shoots of LDI trees (-2.583 MPa) were more negative when compared to immature shoots from LDI trees (-1.630 MPa; Table 3-7). This interaction was absent in Season Two.

Osmotic potential at incipient plasmolysis is variable and can depend on environmental conditions such as temperature and wind speed. Plants will often increase solute concentrations within cells to maintain Ψ_p in plant cells during periods of stress. Osmotic adjustment is the accumulation of solutes in cell vacuoles (Kramer and Boyer, 1995). Many studies have shown that osmotic adjustment is a response to water

stress in plants (Osonubi and Davies, 1978; Koppenaal, et al., 1991; and Meier, et al., 1991). Despite frequent irrigation cycling for FI trees in Season One, and FI and $LDI_{2\text{-}Daily}$ in Season Two, immature shoots of Chinese elm had the most negative $\Psi\pi_{IP}$ both seasons. In addition, visible wilt was noticed for some immature shoots of Chinese elm during Season Two. Immature growth is known for having poor control of guard cells and stomatal aperture, leaving trees vulnerable to increased transpiration (Kirkham, 2005). It is possible that slight to mild water stress due to poor stomatal control may have triggered some osmotic adjustment in Chinese elm which could account for more negative $\Psi\pi_{IP}$. Values measured for $\Psi\pi_{IP}$ in this study were similar to previously cited literature. Measurements of -1.37 and -1.84, -1.30, -1.62 to -1.77, and -0.99 to -2.00 MPa have been reported for expanding and mature leaf tissue of 'Colt' cherry, mature terminal shoots of *U. parvifolia*, mature leaves and shoots of *Q. alba* seedlings, and *Q. ellipsoidalis*, respectively (Abrams, 1988a; Parker and Pallardy, 1985; Parker and Pallardy, 1987; Ranney et al., 1991).

In Season One there was a three-way interaction between species, irrigation regime, and shoot age for P_{max} (Table 3-8). Similar patterns occurred across seasons in regards to shoot age, with larger P_{max} values measured for mature shoots over immature shoots (Table 3-8 and Table 3-18). In Seasons One and Two, P_{max} calculated for mature shoots were double those calculated in immature shoots, with little variation between mature shoot means in Season One (Table 3-8 and Table 3-18). There was no difference in P_{max} between irrigation regimes for Season Two.

Maintenance of turgor is important for plants because changes in Ψ_p can cause changes in cellular content and volume within cells (Kirkham, 2005). Although turgor

pressure is one of the major forces in plant growth, few studies could be located in which turgor was reported. One such study by Beeson (1994) calculated values of 2.5 MPa in of *Quercus virginiana*. While conditions of that study were extreme and not comparable to this study, it indicates live oak is a highly drought tolerant species. It also suggests tissue of live oak may be highly lignified in order to withstand Ψ_p of that magnitude. This insight coupled with the higher SWC_{IP} in Season One supports less plasticity of live oak shoots when compared to shoots of Chinese elm.

Mature shoots (10.366 to 10.473 MPa) had a greater bulk modulus of elasticity (E_o) compared against immature shoots (3.270 to 3.641 MPa) for both Seasons (Table 3-9). In Season Two, live oak (4.975 MPa) had slightly higher E_o than Chinese elm (4.260 MPa), and $LDI_{2\text{-}Daily}$ trees (2.407) had a greater E_o than FI trees (1.498 MPa). Low E_o estimates indicates flexibility of cell walls, which aids in the ability of immature tissue being able to elongate and grow (Nobel, 2009). Values reported in this study are consistent with previously cited literature. Ranney et al. (1991) reported lower values of E_o for expanding leaves (7.92 MPa) compared to mature leaves (10.23 MPa) of 'Colt' cherry. Values of 8.73 MPa have been reported for leaves and shoots of *Q. alba* (Parker and Pallardy, 1987) and 9.15 MPa for shoots of *U. parvifolia* (Ranney et al., 1990).

Similar trends were found between seasons for values of maximum modulus of elasticity (E_{max}). Across seasons, E_{max} was larger for mature shoots compared to immature shoots, and E_{max} was greater for live oak than Chinese elm (Table 3-10). However unlike in Season One, E_{max} varied among irrigation regimes. Maximum modulus of elasticity for LDI trees (2.41 MPa) was higher than FI trees (1.50 MPa).

Maximum modulus of elasticity measurement is a measure of the rigidity of the plant tissue (Nobel, 2009). Parker and Pallardy (1985) reported similar values (2.45 MPa) for leaves of *J. nigra*.

Shoot Elongation Rate

Few studies have reported short-term, diurnal shoot growth rates, and of those conducted there appears to be great variability in growth rates among species. Borchert (1976) measured pin oak sapling growth rates of 0.7917 mm h^{-1}. Reich et al. (1980) measured elongation of stem height rates from 0.0164 to 0.0424 mm h^{-1} in blackjack oak seedlings. Elongation rates of Chinese elm (0.296 mm hr^{-1}) and Live oak (0.208 mm hr^{-1}) when averaged over FI and LDI irrigation regimes were both lower when compared to pin oak saplings, but higher when compared to stem height of backjack oak seedlings.

Across both Seasons, frequently irrigated (FI) Chinese elm elongated at higher rates than other trees. Similarly, LDI and FI irrigation regimes of live oak trees produced comparable growth rates each season. This suggests shoot elongation of live oak was less dependent on irrigation regime than Chinese elm. LDI in Season One was irrigated only once per day. Greater sensitivity of Chinese elm shoot growth being more negative Ψ_w, than that of live oak is found in Season Two Exp. 2. Chinese elm elongation rates were greatest under conditions imposed by the $LDI_{2\text{-}Daily}$ with nighttime elongation rates under Max-night irrigation being the lowest (Table 3-13). In both seasons, overall growth rates were similar between day and night within irrigation regime and species, with the exception of nighttime LDI in Chinese elm. (Table 3-11).

Higher rates of elongation were often associated with Chinese elm trees when under non-water limiting irrigation regimes. This coupled with low measured values of

SWC_{IP},$P_{max,}$ E_o, E_{max}, in both seasons, and in contrast to high reported values for Ψ_p in live oak indicates that shoots of Chinese elm are highly plastic. Reported values of high Ψ_p within plant shoots of live oak may be indicative of high lignification or another less plastic substance. This suggests shoots are less plastic, which was true of species in this study. Given this information and the lower SWC_{IP} in Chinese elm, it is hypothesized that Chinese elm shoots may be more plastic than live oak and that this higher plasticity led to greater shoot elongation under well-watered conditions.

Turgor pressure must be maintained for plant growth to occur, and turgor pressure is mediated, in part, by plant and substrate water status (Anderson and Brodbeck, 1988; Kramer and Boyer, 1995; Ripullone et al., 2009). When plants experience water stress, water uptake may slow and growth may cease in response to lower water potentials and a loss of turgor pressure (Lockhardt, 1965). Zwack et al. (1998) reported that leaf elongation was lower for drought stressed Freeman maple cultivars (19 to 87 cm for drought and control trees, respectively). While trees here were not water stressed to the point of termination of growth rates, patterns for this data were comparable, with highest shoot elongation for trees irrigated to excess and lowest for trees experiencing a water deficit (*i.e*., FI> LDI>LLI).

Shoot elongation in Chinese elm appears to be sensitive to irrigation regime; whereas live oak shoot elongation is not. Beeson and Haydu (1995) reported similar growth in live oak regardless of increased volume of irrigation or increase in cycle above a certain minimum level. However, multiple irrigation regimes applied in sub-volumes throughout the day have been found to optimize growth rates for some species. Beeson (1992) showed *Rhododendron* sp. and *Elaeagnus pungens* cyclically irrigated

to 100% container capacity produced significantly greater growth than plants overhead irrigated once per day. Cyclic irrigation also increased rates of height growth and trunk diameter in *Magnolia grandiflora* compared to plants irrigated once per day (Beeson and Keller, 2003). Given the large difference of Chinese elm growth rates between FI and LLI, Chinese elm may require increased frequency and volume of water application during irrigation to optimize growth rates as well.

Relation of Turgor Pressure to Shoot Growth

For Season One and Season Two Exp. 1, $\Psi_{P\text{-}Norm}$ elongation rates were greater during the daytime and independent of species within well-watered irrigation regimes (FI, LDI, $LDI_{2\text{-}Daily}$). These rates were always highest in Chinese elm irrigated in-excess of container capacity at mid-morning and mid-afternoon, and shortly after sunset (FI) in Season One. Greater elongation rates of elm were also found in Season Two (Exp. 1) independent of irrigation regime. Elm shoot elongation both during the day and at night was greater than at either time of day for live oak. This is likely because there was little different between the FI and $LDI_{2\text{-}Daily}$ regimes. Both applied irrigation during the mid-afternoon and re-saturated containers at midnight. The main different was the quantity applied in the middle of the day, excess verse ~50% of ET_A. When irrigation was restricted to only midnight (LDI) in Season One, both the FI and LDI regimes applied to live oak produced greater elongation rates than that of elms. This suggests easily availability water was more critical to shoot growth of Chinese elm than for live oak. Easily available water is considered that held in a container substrates at matric potentials less than 5 kPa (Beardsell et al., 1979; Bunt, 1983). Chinese elm appears to have a more plastic nature when compared to live oak, as indicated by lower measured SWC_{IP} and lower bulk and maximum moduli of elasticity. Lower values of SWC_{IP}

suggest these shoots may have been more susceptible to water loss and may be more susceptible to water loss than other plant material measured. Furthermore, higher osmotic potential at incipient plasmoysis was found both seasons and observation of wilt was seen in Season Two for immature shoots of Chinese elm. Both of these indicate that immature flushes of Chinese elm may have osmotically adjusted in order to maintain turgor pressure at lower water potential. Wilting was never apparent in immature growth of live oak and higher osmotic potentials at incipient plasmolysis was only apparent in immature shoots of live oak for one season.

In Season Two, three irrigation regimes were applied in an attempt to manipulate Ψ_P both overall and during the night time. As discussed above, the $LDI_{2\text{-Daily}}$ regime was considered optimum for promoting maximum shoot elongation (Beeson and Haydu, 1995). The Min-night regime was hypothesized to promote high Ψ_w and therefore maximum Ψ_P during the nighttime by re-saturating the substrate shortly after stomata closure, as indicated by Figures 3-1 and 3-2. Here FI trees had almost identical Ψ_x by sunset and sunrise the next morning. The Max-night was hypothesized to be the opposite of the Min-night. By re-saturating the container substrate only at dawn, trees would come to equilibrium when stomata closed at sunset with substrate available water approximately half depleted by ET_A during the day. These hypothesized lower Ψ_w should have caused lower Ψ_P throughout the night until the container was re-saturated at dawn. These hypothesized effects were achieved as seen in Figs. 3-1 (oak) and 3-2 (elm). However, statistical analysis was not performed for any values graphed, and without these analyses only possible trends may be reported. Similar trends were observed for Min-night and $LDI_{2\text{-Daily}}$ irrigation. At midnight and dawn, values appeared

to be similar, with high Ψ_p resulted from lower Ψ_w. Whereas for the Max-night irrigation, high Ψ_p also resulted from lower Ψ_w, but values were higher at dawn than those of midnight for both parameters. Turgor pressure was lost in both species around midday with, Ψ_w for Min-night around -1.6 to -1.9 MPa for live oak and Chinese elm respectively. Values for Max-night and $LDI_{2\text{-}Daily}$ were less negative around -1.25 to -1.5 MPa for live oak and Chinese elm, respectively. Water potential and turgor pressure values changed little between sunset to dawn. Species responses appeared to be similar with the exception of longer durations of minimum values close to zero for Ψ_p for Chinese elm.

Despite differences in Ψ_p during Exp. 2, especially during the night time, $\Psi_{P\text{-}Norm}$ elongation rates for Chinese elm were greater during the day than at night (Table 3-14). However for live oak, when separated by irrigation regime, there were no differences in $\Psi_{P\text{-}Norm}$ elongation rates between day and night. Thus shoot elongation in live oak was directly related to turgor pressures. The less negative the diurnal water potential due to irrigation timing, the greater the $\Psi_{p\text{-}Norm}$ growth rate (Fig. 3-1). However for Chinese elm, which appears more sensitive to substrate water availability, $\Psi_{P\text{-}Norm}$ daytime growth was clearly superior to nighttime growth, even though estimated Ψ_p was zero or less for many hrs during the mid-afternoon (Fig. 3-2). These differences are proposed due to low thresholds of Ψ_p above which there was no measurable increase in shoot elongation. In Chinese elm, Ψ_p was higher in shoots during the night than during day. Dividing similar shoot elongation rates (mm hr^{-1}) by higher Ψ_p calculated at night, results in lower $\Psi_{P\text{-}Norm}$ elongation rates (mm MPa-hr^{-1}) at night even though actual elongation rate is similar. Thus it is hypothesized that thresholds for maximum growth of Chinese

elm lie far below Ψ_p calculated here at night. This is probably due to increased plasticity of immature Chinese elm shoots as indicated by lower SWC_{IP} and E_o. It is also possible that Chinese elm and live oak undergo different processes during cell wall expansion as dictated by the composition of their respective cell walls. Cosgrove (2011) suggested that differences in plasticity may be dependent on characteristics of the cell wall such as the number and bundling of cellulose microfibrils in wall cross sectional areas; orientation of the microfibrils relative to the direction of extension; and the density, hydration, and cross linkage of the matrix. This coupled with differences in immature cell wall plasticity may attribute to differences in shoot elongation rates and the role of turgor pressure in growth of these two species. Further pursue of shoot elongation rates under mild water stress may tease out more accurate values for these threshold Ψ_p for maximum shoot elongation in Chinese elm.

Expected outcomes of this study were two fold. The first being possible changes to irrigation scheduling for both the species. The second is new physiological knowledge in regards to growth rates, turgor pressure, and possibly cell wall-loosening mechanisms.

First, results from this study indicate these species likely require different irrigation schedules. Shoot elongation of Chinese elm trees was highly dependent on irrigation volume and frequency, indicating that increased irrigation will result in greater shoot elongation and more marketable plants for tree nurseries. Live oak had little increase in shoot elongation rate between frequently irrigated (3 times daily) and twice-daily irrigated ($LDI_{2\text{-}Daily}$) regimes. This indicates that increased frequency and volume did not result in subsequent increases in shoot elongation, which indicate that increased

irrigation is superfluous. Therefore, increased irrigation will only result in increased water usage and higher, unnecessary costs for nurseries.

Furthermore, this research increases the understanding of shoot elongation and how it relates to turgor pressure. First, quantification of straight shoot elongation measurements was important given that few studies have presented this information. Second, turgor pressure thresholds were indicated, implying that high nighttime turgor pressures may not be the only forces promoting shoot elongation for these two species. Differences found here are indicative of more plastic tissue in immature shoots of Chinese elm shoots compared to live oak and/or differences in cell wall-loosening processes. Further study would need to confirm either of these two possibilities. However, cell wall extensibility may be hard to measure based on current methods of quantification for cell wall mechanics and cell wall-loosening.

LIST OF REFERENCES

Abrams, M.D. 1988a. Comparative water relations of three successional hardwood species in Wisconsin. Tree Physiol. 4:263-273.

Abrams, M.D. 1988b. Sources of variation in osmotic potentials with special reference to North American tree species. For. Sci. 34:1030-1046.

Abrams, M.D. 1990. Adaptations and response to drought in *Quercus* species of North America. Tree Physiol. 7:227-238.

Abrams, M.D.and A.K. Knapp. 1987. Seasonal water relations of three gallary forest hardwood species in northeastern Kansas. For. Sci. 32:687-696.

Abrams, M.D., J.C. Schultz, and K.W. Kleiner. 1990. Ecophysical responses in mesic versus xeric hardwood species to an early-season drought in central Pennsylvania. For. Sci. 36:970-981.

Acevedo, E., E. Fereres, T.C. Hsiao, and D.W. Henderson. 1979. Diurnal Growth Trends, Water Potential, and Osmotic Adjustment of Maize and Sorghum Leaves in the Field. Plant Physiol. 64:476-480.

Anderson, P.C.and B.V. Brodbeck. 1988. Net CO2 assimilation plant water relations characteristics of pecan growth flushes. J. Am. Soc. Hort. Sci. 133:444-450.

Andrade, J.L., F.C. Meinzer, G. Goldstein, F.C. Holbrook, J.C. Cavelier, P. Jackson, and K. Silvera. 1998. Regulation of water flux through trunks, branches, and leaves in trees of a lowland tropical forest. Oecologia 115:463-471.

Anselmi, S., M. Chiesi, M. Giannini, F. Manes, and F. Maselli. 2004. Estimation of Mediterranean forest transpiration and photosynthesis through the use of an ecosystem simulation model driven by remotely sensed data. Global Ecol. Biogeogr. 13:371-380.

Bahari, Z.A., S.G. Pallardy, and W.C. Parker. 1985. Photosynthesis, water relations, and drought adaptations in six woody species of oak-hickory forests in central Missouri. For. Sci. 31:557-569.

Beardsell, D.V., D.G. Nichols, and D.L. Jones. 1979. Physical properties of nursery potting-mixtures Scientia. Hortic. 11:1-8.

Beeson, R.C. 1992. Restricting overhead irrigation to dawn limits growth in container grown woody ornamentals. HortScience 27:996-999.

Beeson, R.C. 1994. Water relations of field-grown *Quercus virginiana* Mill. from pre-harvest through containerization and 1 year into a landscape. J. Amer. Hortic. Sci. 119:169-174.

Beeson, R.C. 2011. Weighing lysimeter systems for quantifying water use and studies of controlled water stress for crops grown in low bulk density substrates. Agr. Water Manage. 98:967-976.

Beeson, R.C.and E.F. Gilman. 1992. Water stress and osmotic adjustment during post-digging acclimation of *Quercus virginiana* produced in fabric containers. J. Amer. Hortic. Sci. 10:208-214.

Beeson, R.C.and J. Haydu. 1995. Cyclic microirrigation in container-grown landscape plants improves plant growth and water conservation. J. Environ. Hort. 13:6-11.

Beeson, R.C.and K. Keller. 2003. Effect of cyclic irrigation on growth of magnolias produced using five in-ground systems. J. Environ. Hort. 21:148-152.

Begg, J.E.and N.C. Turner. 1970. Water potential gradients in field tobacco. Plant Physiol. 46:343-346.

Bonner, J.and J.E. Varner. 1976. Plant biochemistry. Academic Press, New York.

Borchert, R. 1976. Differences in shoot growth patterns between juvenile and adult trees and their interpretation based on systems analysis of trees. Acta. Hort. 56:123-130.

Brockman, C.F. 2001. Trees of North America: A Guide to Field Identification. Golden Guides from St. Martin's Press, New York.

Bunt, A.C. 1983. Physical properties of mixtures of peat and minerals of different particles sizes and bulk density for potting substrates. Acta. Hort. 150:143-153.

Burgert, I. 2006. Exploring the micromechnaical design of plant cell walls. Am. J. Bot. 93:1391-1401.

Burough, I. 1980. Gas analyzer and gas analyzing. In: U.S.P. Office (Ed., Google Patents,July 19, 2010. Andros Inc., Berkeley, CA, United States of America, pp. 1-7.

Carpita, N.C.and D.M. Gibeaut. 1993. Structural models of primary cell walls in flowering plants: Consistency of molecular structure with the physical properties of the walls during growth. Plant J. 3:1-30.

Cline, R.C.and G.S. Campbell. 1976. Seasonal and diurnal water relations of selected forest species. Ecology 57:367-373.

Corcuera, L., J.J. Camarero, and E. Gil-Pelegrin. 2002. Functional groups in *Quercus* species dervied from the analysis of pressure-volume curves. Trees 16:465-472.

Cosgrove, D.I. 1989. Characterization of long-term extension of isolated cell walls from growing cucumber hypocotyls. Planta 177:121-130.

Cosgrove, D.I. 1993. Wall extensibility: It's nature, measurement, and relationship to plant cell growth. New Phytol. 124:1-23.

Cosgrove, D.I. 2011. Measuring *in vitro* extensibility of growing plant cell walls. vol. 715. Humana Press, New York.

Cullina, W. 2002. Native trees, shrubs, and vines: a guide to using, growing, and propagating North American woody plants. Houghton Mifflin Company, Boston.

Cutler, J.M., P.L. Steponkus, M.J. Wach, and K.W. Shahan. 1980. Dynamic Aspects and Enhancement of Leaf Elongation in Rice. Plant Physiol. 66:147-152.

Danilov, M.D. 1954. Diurnal periodicity in the growth and shoots of some tree and shrub species. Doklady Akad. Nauk. S.S.S.R. 96:205-208.

Dreyer, E., F. Bousquet, and M. Ducrey. 1990. Use of pressure volume curves in water relation analysis on woody shoots: Influence of rehydration and comparison of four European oak species. Ann. For. Sci. 47:285-297.

Durkovic, J., I. Canova, T. Priwitzer, M. Biroscikova, P. Kapral, and M. Saniga. 2010. Field assessment of photosynthetic characteristics in micropropagated and grafted wych elm (*Ulmus glabra* Huds.) trees. Plant Cell Tiss. Org. 101:221-228.

Fielding, J.M. 1955. The seaonsal and daily elongation of the shoots of Monterey pine and the daily elongation of the roots. Forestry & Timber Bur. Australia 75.

Fort, C., M.L. Fauveau, F. Muller, P. Label, A. Granier, and E. Dreyer. 1997. Stomatal conductance, growth and root signaling in young oak seedlings to partial soil drying. Tree Physiol. 17:281-289.

Franks, P.J., P.L. Drake, and R.H. Froend. 2007. Anisohydric but isohydrodynamic: Seasonally constant plant water potential gradient explained by a stomatal control mechanism incorporating variable plant hydraulic conductivity. Plant, Cell Environ. 30:19-30.

Fry, S.C. 1989. The structure and function of xyloglucan. J. Exp. Bot. 40:1-11.

Fry, S.C., R.C. Smith, K.F. Renwick, D.J. Martin, S.K. Hodge, and K.J. Matthews. 1992. Xyloglucan endotransglycosylase, a new wall-loosening enzyme activity from plants. Biochem. J. 282:821-828.

Gallego, H.A., M. Rico, G. Moreno, and I. Santa Regina. 1994. Leaf potential and stomatal conductance in *Quercus pyrenaica* Willd. forests: Vertical gradients and responses to environmental factors. Tree Physiol. 14:1039-1047.

Geitmann, A. 2006. Experimental approaches used to quantify physical parameters at cellular and subcellular levels. Am. J. Bot. 93:1380-1390.

Geitmann, A.and J.K.E. Ortega. 2009. Meachnics and modeling of plant cell growth. Trends Plant Sci. 14:467-478.

Gu, M., C.R. Rom, J.A. Robbins, and D.M. Oosterhuis. 2007. Effect of water deficit on gas exchange, osmotic solutes, leaf abscission, and growth in four birch genotypes (*Betula* L.) under a controlled environment. HortScience 42:1383-1391.

Hager, A., H. Menzle, and A. Krauss. 1971. Experiments and hypothesis of the primary effect of auxins on expansion growth. Planta 100:47-75.

Haldimann, P., A. Galle, and U. Feller. 2008. Impact of an exceptionally hot dry summer on photosynthetic traits in oak (*Quercus pubescens*) leaves. Tree Physiol. 28:785-795.

Hsiao, T.C.and E. Acevedo. 1974. Plant responses to water deficits, water use-efficiency, and drought resistance. Agr. Meteorol. 14:59-84.

Hsiao, T.C., E. Acevedo, E. Fereres, and D.W. Henderson. 1976. Water stress, growth, and osmotic adjustment. Philosophical Transactions of the Royal Society of London B, Biological Sciences 273:479-500.

Husken, D., E. Steudle, and U. Zimmermann. 1978. Pressure probe technique for measuring water relations of cells in higher plants. Plant Physiol. 61:158-163.

Kandiko, R.A., R. Timmis, and J. Worrall. 1980. Pressure-volume curves of shoots and roots of normal and drought conditioned western hemlock seedlings. Can. J. For. Res. 10:10-16.

Kirkham, M.B. 2005. Principles of soil and pane water relations. Elsevier Academic Press, Boston.

Koch, G.W., J.S. Amthor, and M.L. Goulden. 1994. Diurnal patterns of leaf photosynthesis, conductance, and water potential at the top of a lowland rain forest canopy in Cameroon: Measurements from the *Radeau des Cimes*. Tree Physiol. 14:347-360.

Koriba, K. 1958. On the periodicity of tree growth in the tropics, with reference to the mode of branching, the leaf fall, and the formation of resting buds. Gard. Bull. 17:11-81.

Korner, C.and P.M. Cochrane. 1985. Stomatal responses and water relations of *Eucalyptus pauciflora* in summer along an elevational gradient. Oecologia 66:443-455.

Kozlowski, T.T. 1964. Shoot growth in woody plants. Bot. Rev. 30:335-392.

Kozlowski, T.T. 1982. Water supply and tree growth. Commonw. Forest. Bur. 43:57-95.

Kramer, P.J. 1943. Amount and duration of growth of various species of tree seedlings. Plant Physiol. 18:239-251.

Kramer, P.J.and J.S. Boyer. 1995. Water relations of plants and soils. Academic Press, San Diego.

Kwon, K.W.and S.G. Pallardy. 1989. Temporal changes in tissue water relations of seedlings of *Quercus acutissima*, *Q. alba*, and *Q. stellata* subjected to chronic water stress. Can. J. For. Res. 19:622-626.

Lambers, H., F.S. Chapin, and T.L. Pons. 2008. Plant physiological ecology. Springer, New York.

Larcher, W. 1980. Physiological plant ecology. Springer-Verlag, Berlin.

Lockhardt, J.A. 1965. Plant biochemistry. Academic Press Inc, New York.

Lotan, J.E.and R. Zahner. 1963. Shoot and needle responses of 20-year-old red pine to current soil moisture regimes. For. Sci. 9:497-506.

Maccubbin, T.and G.B. Tasker. 1997. Florida gardener's guide. Cool Springs Press, Franklin, Tennessee.

Maier-Maercker, U. 1998. Dynamics of change in stomatal response and water status of *Picea abies* during a pesistant drought period: A contribution to the traditional view of plant water relations. Tree Physiol. 18:211-222.

Mazzoleni, S.and D.I. Dickmann. 1988. Differential physiological and morphological responses of two hybrid Populus clones to water stress. Tree Physiol. 4:61-70.

McQueen-Mason, S.and D.I. Cosgrove. 1994. Disruption of hydrogen bonding between plant cell wall polymers by proteins that induce wall extension. Proc. Natl. Acad. Sci. USA 91:6574-6578.

Meier, C.E., R.J. Newton, J.D. Puryear, and S. Sen. 1992. Physiological responses of Loblolly Pine (*Pinus taeda* L.) seedlings to drought stress: Osmotic adjustment and tissue elasticity J. Plant Physiol. 140:754-760.

More, D.and J. White. 2002. The illustrated encyclopedia of trees. Timber Press, Portland.

Mork, E. 1941. Om sambandet mellom temperature og. Nekst. Medd. Det Norske Skogforsoksvesen 8:1-89.

Myers, B.J. 1988. Water stress integral-a link between short-term stress and long-term growth. Tree Physiol. 4:315-323.

Niu, G., D.S. Rodriguez, and W. Mackay. 2008. Growth and physiological responses to drought stress in four oleander clones. J. Amer. Hortic. Sci. 133:188-196.

Nobel, P.S. 2009. Physicochemical and environmental plant physiology. Academic Press, Boston.

Omae, H., A. Kumar, K. Kashiwaba, and M. Shono. 2007. Assessing drought tolerance of snap bean (*Phaseolus vulgaris*) from genotypic differences in leaf water differences in leaf water relations, shoot growth and photosynthetic parameters. Plant Prod. Sci. 10:28-35.

Parker, W.C.and S.G. Pallardy. 1985. Genotypic variation in tissue water relations of leaves and roots of black walnut (*Juglans nigra*) seedlings. Physiol. Plant. 64:105-110.

Parker, W.C.and S.G. Pallardy. 1987. The influence of re-saturation method and tissue type on pressure-volume analysis of *Quercus alba* L. seedlings. J. Exp. Bot. 38:535-549.

Parker, W.C.and S.G. Pallardy. 1988. Leaf and root osmotic adjustment in drought-stressed *Quercus alba*, *Q. macrocarpa*, and *Q. stellata* seedlings. Can. J. For. Res. 18:1-5.

Ranney, T.G., N.L. Bassuk, and T.H. Whitlow. 1991. Turgor maintennance in leaves and roots of 'Colt' cherry trees (*Prunus avium* x *pseudocerasus*) in response to water stress. J. Hortic. Sci. 66:381-387.

Ranney, T.G., T.H. Whitlow, and N.L. Bassuk. 1990. Response of five temperate deciduous tree species to water stress. Tree Physiol. 6:439-448.

Raper, C.D.and P.J. Kramer. 1983. Crop reactions to water and temperature stresses in humid, temperate climates: Westview special studies in agriculture/aquatic science and policy. Westview Press, Boulder, CO.

Raven, P.H., R.F. Evert, and S.E. Eichhorn. 2005. Biology of plants. W.H. Freeman and Company, New York.

Rayle, D.and R.E. Cleland. 1970. Enhancement of wall loosening and elongation by acid solutions. Plant Physiol. 46:250-253.

Reich, P.B., R.O. Teskey, P.S. Johnson, and T.M. Hinckley. 1980. Periodic root and shoot growth in oak. For. Sci. 26:590-598.

Ripullone, F., M. Borghetti, S. Raddi, E. Vicinelli, R. Baraldi, M.R. Guerrieri, A. Nole, and F. Magnani. 2009. Physiological and structural changes in response to altered precipitation regimes in Mediterranean macchia ecosystem. Trees-Struct. Funct. 23:823-834.

Simpson, G.M. 1981. Water stress on plants. Praeger, New York.

Smith, J.P. 1977. Vascular plant families. Mad River Press Inc., Eureka, CA.

Smith, R.C.and S.C. Fry. 1991. Endotransglycosylase of xyloglucans in plant cell suspension cultures. Biochem. J. 279:529-535.

Steudle, E., U. Zimmermann, and U. Luttge. 1977. Effect of turgor pressure and cell size on the wall elasticity of plant cells. Plant Physiol. 59:285-289.

Taiz, L. 1994. Expansins: Proteins that promote cell wall loosening in plants. Proc. Natl. Acad. Sci. USA 91:7387-7389.

Taiz, L.and E. Zeiger. 2006. Plant physiology. Sinauer Associates, Inc., Publishers, Sunderland, MA.

Tardieu, F.and T. Simonneau. 1998. Variability among species of stomatal control under fluctuating soil water status and evaporative demand: Modelling isohydric and anisohydric behaviors J. Exp. Bot. 49:419-432.

Taylor, N. 1988. Taylor's guide to trees. Houghton Mifflin Company, Boston.

Turner, N.C. 1988. Measurement of plant water status by the pressure chamber technique. Irrigation Sci. 9:289-308.

Tyree, M.T.and H.T. Hammel. 1972. The measurement of the turgor pressure and the water relations of plants by the pressure-bomb technique. J. Exp. Bot. 23:267-282.

Tyree, M.T.and P.G. Jarvis. 1982. Water in tissues and cells. In: O.L. Lange, P.S. Nobel, C.B. Osmond, and H. Ziegler (Eds.), Encyclopedia of plant physiology (New Series) Springer-Verlag, Berlin, pp. 35-77.

Urban, L., A. Jaffrin, and A. Chraibi. 1993. Analysis of pressure-volume curves of leaves of *Rosa hybrida* cv. Sonia. J. Exp. Bot. 44:605-613.

Wang, Z.C.and G.W. Stutte. 1992. The role of carbohydrates in active osmotic adjustment in apple under water stress. J. Am. Soc. Hort. Sci. 117:816-823.

Watkins, J.V., T.J. Sheehan, and R.J. Black. 2005. Florida landscape plants: Native and exotic. University of Florida Press, Gainesville.

Wullschleger, S.D., K.B. Wilson, and P.J. Hanson. 2000. Environmental control of whole-plant transpiration, canopy conductance, and estimates of the decoupling coefficient for large red maple trees. Agr. Meteorol. 104:157-168.

Xu, B., F. Li, L. Shan, Y. Ma, N. Ichizen, and J. Huang. 2006. Gas exchange, biomass partition and water relationships of three grass seedlings under water stress. Weed Biol. Manag. 6:79-88.

Yacoubi, S., K. Zayani, N. Zapata, A. Zairi, A. Slatni, R. Salvador, and E. Playan. 2010. Day and night time sprinkler irrigated tomato: Irrigation performance and crop yield. Biosyst. Eng. 107:25-35.

Zahner, R. 1962. Terminal growth and wood formation by juvenile loblolly pine under two soil moisture regimes. For. Sci. 8:345-352.

Zwack, J.A., W.R. Graves, and A.M. Townsend. 1998. Lead water relations and plant develpoment of three Freeman maple cultivars subjected to drought. J. Amer. Hortic. Sci. 123:371-375.

BIOGRAPHICAL SKETCH

Emily Elaine Massey was born in Jacksonville, Illinois. In 2008, she received her B.S. from Illinois College in Jacksonville, Illinois with a major in biology/chemistry and a minor in environmental science. While attending Illinois College, she studied symbiotic and asymbioitc orchid propagation at the Orchid Recovery Program under Dr. Lawrence Zettler. Her work centered on propagation and restoration of threatened and rare species from Illinois and south Florida.

In 2009, she continued her ecological based work at the University of Florida in Gainesville, Florida. She received her M.S. from the College of Agriculture and Life Science in 2011. Her work with two popular Florida landscape trees has added to the scientific knowledge of shoot elongation and the effects of turgor pressure on shoot elongation rates. In addition, data collected from this study will be helpful in regulating irrigation cycles for live oak and Chinese elm.

In her free time, she enjoys reading, watching movies, and spending time with her three cats. She is an avid fan of Bob Dylan and playing board games.